UNIVERSITAT POLITÈCNICA DE CATALUNYA

MASTER THESIS

USBL integration and experimental assessment in a multisensor EKF-based AUV navigation approach

Author:
Eric GUERRERO

Supervisors:
Dr. Francisco BONIN
Dr. Cecilio ANGULO

A thesis submitted in fulfillment of the requirements for the degree of Master of Science

in the

Universitat Politècnica de Catalunya
Automatic Control Department

developed at

Universitat de les Illes Balears
Systems, Robotics & Vision Group

October 20, 2016

Acknowledgements

I would like to thank to all the people involved in the Master's degree in Automatic Control and Robotics of the UPC, for the quality of the studies, the interest and the provided motivation. Specially to my thesis supervisor Dr. Cecilio Angulo Bahón for its support and advice, and to all the colleagues whom I have had the opportunity to meet and to work with.

Furthermore, I would like to express my gratitude to all the members of the Systems, Robotics and Vision group of the UIB, for their kind reception. Specially to the underwater robotics team, for the attention and all the great experiences shared together, and in particular to my thesis director Dr. Francisco Bonin Font, for the continuous engagement and cooperation.

Pero sobretodo, quisiera agradecer a mi familia por el cariño y la confinza depositada, nada de esto hubiera sido posible sin vuestra asertiva paciencia.

Agrair també, a les grans amistats que m'envolten, per en conjunt aportar continues dosis d'energia i motivació per afrontar nous reptes.

Contents

List of Abbreviations

AHRS	**A**ttitude **H**eading **R**eference **S**ystem
ASC	**A**utomated **S**urface **C**raft
AUV	**A**utonomous **U**nderwater **V**ehicle
DOF	**D**egree **o**f **F**reedom
DR	**D**ead-**r**eckoning
DVL	**D**oppler **V**elocity **L**og
EKF	**E**xtended **K**alman **F**ilter
ENU	**E**ast **N**orth **U**p
GIB	**G**PS **I**ntelligent **B**uoy
GPS	**G**lobal **P**ositioning **S**ystem
GS	**G**round **S**tation
GT	**G**round **T**ruth
IMU	**I**nertial **M**easurement **U**nit
LAN	**L**ocal **A**rea **N**etwork
LBL	**L**ong **B**ase**l**ine
NED	**N**orth **E**ast **D**own
ROS	**R**obot **O**perating **S**ystem
ROV	**R**emotely **O**perated **V**ehicle
RP3	**R**aspberry **P**i **3**
SLAM	**S**imultaneous **L**ocalization **a**nd **M**apping
SSH	**S**ecure **Sh**ell
SSS	**S**ide **S**can **S**onar
TCP	**T**ransmission **C**ontrol **P**rotocol
TOF	**T**ime **o**f **F**light
UKF	**U**nscented **K**alman **F**ilter
USBL	**U**ltra **S**hort **B**ase**l**ine
VO	**V**isual **O**dometry
WLAN	**W**ireless **L**ocal **A**rea **N**etwork

Chapter 1

Introduction

This Master's Thesis details the practical implantation of an acoustic positioning and communication system in an autonomous underwater vehicle used for research purposes. The implementation has been followed by the evaluation of the system performance. Both, in simulation and in field tests. The purpose of this integration, is to provide an absolute position measurement and a continuous communication link when the robot is underwater, in order to increase the localization accuracy and the robot supervision. It will allow to perform larger and deeper missions, increasing the autonomy of the robot. This chapter presents the project by first exposing the motivation, section 1.1, secondly it enumerates the goals of the project in the section 1.2, and thirdly the research projects in which Thesis is framed, section 1.3. Moreover, an state of the art is presented in the section 1.4, followed by the methodology used, section 1.5.

1.1 Motivation

Underwater robotics is an increasing focus of research that provides the opportunity to explore the oceans saving resources and time. It improves our understanding about several fields for environmental protection and nowadays it permits to monitor variations in water characteristics such as salinity, temperature and currents in a very efficient manner, which is useful to improve the performance of the weather forecast models. It also dedicates a main source of research on developing tools to monitor underwater wildlife, to have a better understanding about the population of animals, plants and coral reefs in order to improve the environmental management.

Furthermore, a principal focus of investments in marine technologies is devoted to the exploitation of natural resources such as oil or gas, as well as the military or fishing industry. Whereas the study of wide areas of the sea floor may be done using powerful sonars attached to ships, a more precise result can be obtained by using underwater vehicles able to move close to the sea bottom. The increasing performance and the reduction of size of electronic devices together with the continuous innovations in computer science is making robotics accessible for multiple tasks.

Many kinds of underwater vehicles exist, while for exploration or inspection the use of Autonomous Underwater Vehicles (AUV) allows more complex and deeper missions, Remotely Operated Vehicles (ROV) are also used. The basic difference between an AUV and a ROV is the navigation, whereas an AUV has an autonomous navigation system based in the self localization and the decision of the trajectory path, a ROV is always teleoperated from a surface vessel. In the case of the ROVs, a wired connection is used to support the huge sensor data flow that has to arrive to the operator. In contrast, AUVs need a vessel only for deployment and collection. The reduction on operational costs is making the research community step forward full autonomous robots able to follow high-level commands.

In order to be autonomous, a vehicle needs to have a perception of the surrounding environment in which it navigates, it is required to have an accurate localization in order to have a fair navigation and well referenced sensor data. For example, exploration applications require the mapping of the environment in the form of 2D or 3D reconstructions. Since the map creation depends on the sensor observations and on the robot localization, the estimation of accurate robot positions is a key issue to obtain consistent and accurate maps allowing the robot to perform different autonomous tasks.

An accurate localization is the result of the combination of a set of sensors providing pose and odometry measurements and a filter which produces a position estimation based on the fusion of all the input lectures. Traditional techniques such as Dead-Reckoning (DR), based the position estimation on the odometry provided by proprioceptive sensors such as inertial, magnetic and pressure sensors, which are prone to error accumulation. Adding more complex exteroceptive sensors such as a Doppler Velocity Log (DVL), which provides linear speed estimations, seems to bound the error rate but not the drift, being the drift of the order of the 2% of the traveled distance.

Most modern AUVs aid DR estimation with DVL and absolute positioning systems in order to bound the trajectory error. Such a system is often called aided inertial navigation system (AINS). Due to the slow rate of existing absolute positioning systems DR sensors are still being the core of the position estimation, providing a movement estimation that might be integrated to produce a continuous pose estimation well suited for the navigation and control of a robot.

By definition absolute position can not be obtained using odometric sensors which can only measure motion. Even with a well defined starting condition, the estimated pose obtained from the integration of velocity and acceleration measurements may accumulate error due to measurement noise. Absolute positioning systems are usually based on acoustic technology: in fact, they are based on the time of flight of acoustic signals between different transponders, section 2.5. Other techniques based on bottom tracking, such as the visual based SLAM have been shown to provide accurate results, but many trajectory restrictions and sea bottom characteristics are required.

Acoustic positioning systems have the advantage that they can be also used for communications. Although a wired connection is usual for AUV testing, a non wired communication system is a key factor for further improvement and development of autonomous tasks as well as enlarging the working environment. Underwater communication is important not only to guarantee a proper human supervision of the robot safety, but also to be able of sharing information with other vehicles and perform cooperative navigation.

The USBL (Ultra-Short Baseline) technology was presented as a promising solution for underwater communication and localization. It is considered as small sized and easy deployed system compared to it's acoustic positioning systems counterparts. To sum up, the USBL increases the capabilities of a robot: it provides an absolute position measurement that bounds the trajectory error, and it enables non-wired underwater communications. It contributes to the development of deeper and larger missions with a proper vehicle supervision.

1.2 Objectives

The main contribution of this thesis is twofold: to provide an non-wired underwater communication system, and to implement an absolute positioning system able to bound the trajectory error of the Turbot AUV presented in section 2.2.1. Moreover, the precision of the developed positioning system will be evaluated in a real environment.

Several objectives are framed into this project, all of them related with the implementation of acoustic communications, processing of absolute delayed position measurements, multisensor fusion, and evaluation through experimental testing.

1. **Communication**
    - Device driver.
    - Acoustic link.
2. **Measurements**
    - Set up device parameters.
    - Filter outliers.
    - Evaluate precision.
3. **Fusion**
    - Update delayed measurements.
    - Integrate position in a Kalman based filter.
4. **Evaluation**
    - Simulation
    - Field tests

The communications block will deal with the development of a communication layer able to interact between the acoustic device and the robotic software architecture based on the Robot Operating System (ROS).

In order to get a position estimate, the measurements of the acoustic positioning system will be filtered to get rid of outliers, and a precision evaluation will be performed to estimate the noise present on the measurements. Since the acoustic communications suffer from high latency, the acoustic position estimate will have a delay of the order of seconds which will have to be corrected before being integrated in an estimation filter. Finally the performance of the developed system will be validated in simulation and evaluated in field test at the sea. In addition, two different Kalman based filter techniques will be compared, the Extended Kalman Filter (EKF) and the Unscented Kalman Filter (UKF), in order to see which provides better results for such a multisensor system.

1.3 Scope

A precise AUV localization is needed for several marine applications. This project is framed in the context of two Spanish national projects MERBOTS/SUPERION (DPI2014-57746-C3) Ridao, 2016 and ARSEA (TIN2014-58662-R) Burguera, 2016a.

MERBOTS/SUPERION The MERBOTS (DPI2014-57746-C3) project is focused on the use of three heterogeneous vehicles to conduct an intervention mission cooperatively in different configurations at different phases. It has the main goal of increasing the safety and reduce the cost of underwater intervention missions. In a first stage one AUV performs a 3D mapping using a side scan sonar (SSS) bathymetry, being globally positioned by an Autonomous Surface Craft (ASC). Then, in a second stage, another AUV surveys an smaller goal area selected from the bathymetry to perform a more refined and accurate 3D reconstruction using stereo imagery. Moreover, the stereo imagery is used for object detection and intervention planning. Finally, in a third stage, a ROV vehicle, equipped with a robotic manipulator arm, is used for intervention, supervised by the stereo pair AUV.

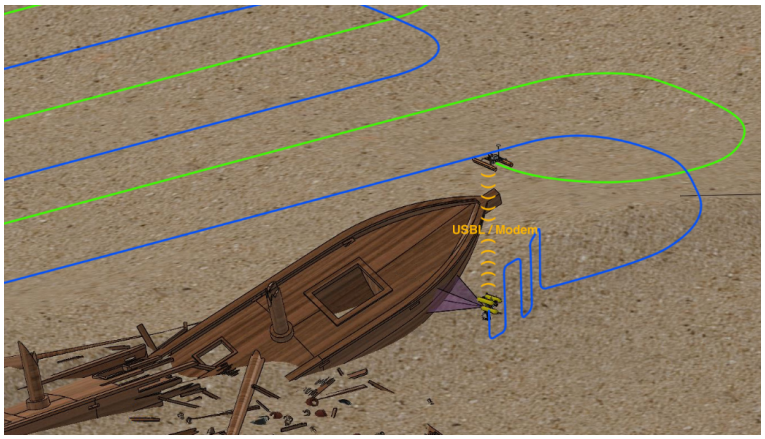

(A) Cooperative survey

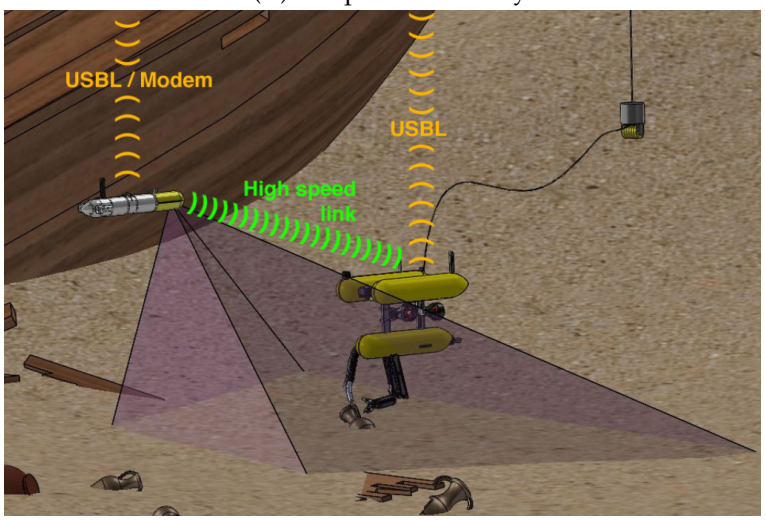

(B) Cooperative intervention

FIGURE 1.1: Images from MERBOTS project

The subproject SUPERION (DPI2014-57746-C3-2-R) is focused on underwater computer vision: 2D/3D reconstruction, object detection and robotic arm supervision.

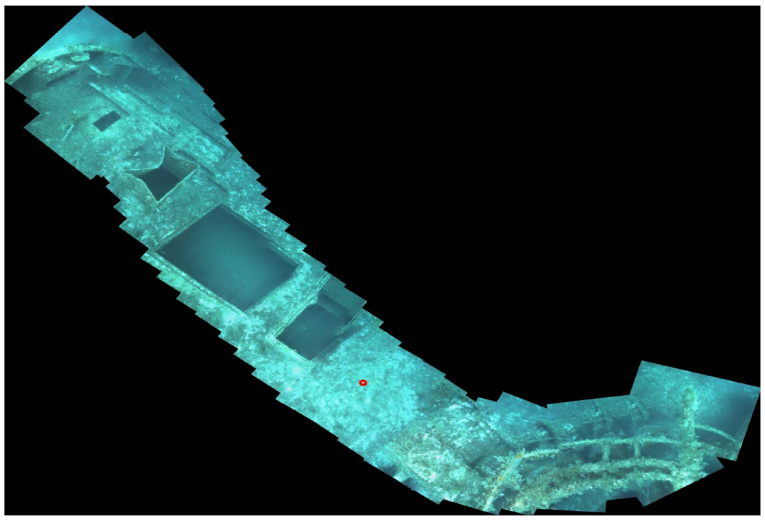

(A) 2D Reconstruction - Mosaic

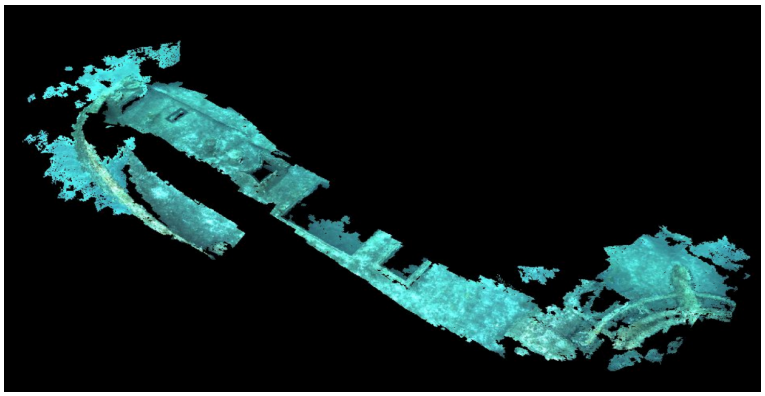

(B) 3D Reconstruction - Pointcloud

FIGURE 1.2: Reconstructions of the Boreas wreck located at the coast of Girona (Spain)

Figure 1.2 shows the 2D and 3D reconstructions of the wreck called Boreas located ad the coast of Girona (Spain), the sequences of images were gathered during the project sea tests performed the past June 2016.

ARSEA The ARSEA (TIN2014-58662-R) project is focused on surveying and controlling areas of special ecological, social or economical interest. For instance, photo-mosaicking or building 3D models of seagrass meadows, ship/aircraft wrecks or deteriorated infrastructures. It has two main goals: one is to develop a new interface to operate ROVs using a 3D representation in which the pilot is able to navigate using a virtual reality headset, the other is to design and implement tools for automatic supervision of marine environments, having as a principal application the classification of the sea bottom coverage.

Many research has been done to obtain the bottom coverage of Posidonia Oceanica (PO) medows. PO is a Mediterranean endemic seagrass strongly related to the health of the coastal ecosystems, and is identified as a natural habitat of priority interest by the European Commission, directive 92/43/CEE. The proposed approach is thought to be more accurate than others that use satellite images or sonar bathymetries duo to the closeness of the data gathering and the image definition.

To compute the bottom coverage of PO, a support vector machine (SVM) is used for area classification, but also a mosaicking algorithm Fidalgo, 2016 to obtain an image of all the explored region, figure 1.3.

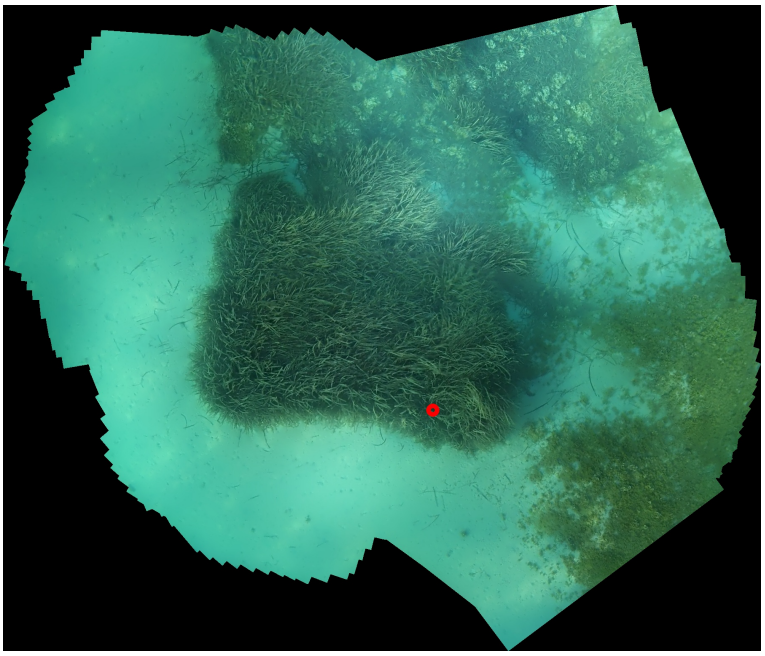

FIGURE 1.3: 2D Reconstruction - Mosaic for Posidonia Oceanica classification

Both projects need accurate position estimates, not only to improve navigation but also to improve scene reconstruction. This will be a must to produce precise and consistent reconstructions of bigger areas with low image feature density.

Many times harsh marine environments make it difficult to find correspondences between images, corrupting the environment reconstructions and producing non-accurate homography transformations. Then, a robust sensorial equipment for localization is critical in order to fed good position estimations and have well referenced sensor data for the mapping algorithms. Also, a communication link between the vehicle and the remote station, or even between different vehicles will be needed.

1.4 State of the art

1.4.1 Communication

Underwater wireless communications are usually established by means of optic or acoustic technology. While optical tech is beginning to get the attention of the research community due to the high transmission rate ($\sim Gbps$) on small range communications, acoustic communications have several features that make them the first option for many underwater applications, being nowadays in a mature development. Kaushal, 2016 provides an exhaustive research on underwater optical wireless communications, providing state of the art specifications of acoustic, radio and light communications. The latter is well suited for short range communications ($\sim 30m$), with possible applications in cooperative robotics . In contrast, the former has a lower transmission rate ($\sim kbps$) and a larger range ($\sim km$). Further added values for acoustic technology are that a positioning measure may be obtained from the time of flight of an acoustic signal. Kebkal, 2012 presents a solution to blend communication and positioning modes of acoustic devices, which provides the possibility of using the same acoustic signal for communication and positioning. It is based on S2C technology for robust communication, Kebkal, 2002, which is able to improve signal resolution by separating multipath arrivals.

1.4.2 Localization

Traditional localization approaches based on dead reckoning (DR), which produces pose estimations only from odometric measurements, are subject to cumulative error that produce a drift on the estimation. Whitcomb, 1999 presents a technique to bound the AUV pose error. It proposes a DR position estimation aided by a Doppler velocity log (DVL), to improve the odometric estimation, and an acoustic-based absolute positioning system to periodically reset the position error accumulated by the odometry estimation. The author conclude that an absolute measurements provide a robust estimation and compensate possible motion sensor misalignment.

Nowadays many actual AUVs integrate aided inertial navigation systems (AINS), adding more complex exteroceptive sensors to bound the error. That is the case of the Typhoon [1], SeaBED [2], Girona500 [3]. All of them aid DR with DVL sensors and different sources of absolute position measurements: one common characteristic of most modern AUVs is that they obtain a pose estimation from the fusion of multiples types of sensor data. From Rigby, 2006,

> *"Multisensor fusion provides several benefits as improved accuracy, robustness and enhanced resolution. Uncertainty can be reduced by using multiple sources of information, corrupted measurements can be more easily identified and rejected from redundant sensor readings."*

Due to the slow rate of actual absolute positioning systems, DR still being the core of the position estimation. Whereas DVL bounds the error rate, it does not bounds the drift. Absolute position measurements have larger noise rates but they do not accumulate error. They can be obtained from several kinds of systems. For instance, the use of visual sensors as a source of absolute positioning is also possible through simultaneous localization and mapping (SLAM) processes. Eustice, 2008 outlines a visual aided navigation approach in a visual based SLAM framework to develop a cheap localization method for near-seafloor navigation. Mur-Artal, 2015, presents a good feature based monocular SLAM implementation approach for general environments. However it may lose performance in underwater environments, due to harsh quality imagery. A novel technique is presented in Negre, 2016, which can be used in feature-poor underwater environments. It consists in a feature clustering for the loop closing detection stage of the SLAM process, with the best tested performance obtained when using the stereoscopic SLAM technique presented in Bonin-Font, 2016. Another example is shown in Chen, 2015, where

[1] Typhoon AUV description. Caiti et al., 2014
[2] SeaBED AUV. https://www.whoi.edu/main/seabed
[3] Girona500 AUV. Ribas, 2012a

the author presents a technique to localize an underwater vehicle by fusing mechanical scanning sonar and DR measurements in a GraphSLAM algorithm.

Long baseline (LBL) and ultra short baseline (USBL) are two examples of acoustic positioning configurations, they are considered the most reliable and versatile systems to provide absolute position fixes when the vehicle is underwater. Philip, 2003a,b,c provide an exhaustive introduction for the evaluation and calibration of this devices. Furthermore, absolute positioning may be obtained from acoustic communication devices using arbitrary configurations, such as underwater sensor networks (UWSN). UWSN fuse wireless communication technology with small sized sensors and intelligent computing, they work as a net of autonomous sensor nodes that might be used for data collection, communication and positioning. Both, Felemban, 2015 and Fengzhong, 2016 present a survey on UWSN using acoustic technology.

1.4.3 Sensor fusion

Since there are many types of sensor data, a major focus of concern consists in processing multisensor data in order to produce an estimation. Nowadays almost all the research is related to probabilistic estimators, most of them based on the methods detailed in Thrun, 2005.

The most extended probabilistic estimation technique was presented by Kalman, 1960. It solved the Wiener problem, Wiener, 1949, of obtaining the specification of a linear dynamic system subject to random noise. The presentation of the currently known as Kalman filter (KF), was the beginning of the use of the probability theory in engineering. Furthermore, a generic solution was developed to extend the use to non-linear models , the extended Kalman filter (EKF), that consists in a first order linearization of the non-linear function through a first order Taylor expansion. This methods provide models for Gaussian random processes described with states and state transitions, and using first order differential equations.

The EKF has been extensively used in robotics as a general solution that results in a fair performance with low process complexity and low memory usage. Nevertheless, there exist other filtering techniques that might be more appropriate to fulfill different requirements, for example the use of delayed measurements or non-Gaussian processes. The selection of a filtering technique will depend on the kind of existing inputs and desired outputs. For example, Julier, 1997 presents the unscented Kalman filter (UKF): a filtering technique that addresses the sub-optimal problem of the EKF. The UKF uses a deterministic sampling approach to carefully select sample points to be propagated through the nonlinear system. It captures more accurately the posterior mean and covariance than the EKF in the presence of non-linear transitions. Wan, 2000 provides a clear comparison between both filtering techniques.

An other well known approach used for state propagation are the particle filters, or Montecarlo methods, Gordon, 1993. In brief, they substitute the Gaussian error distribution, which only has two parameters to transform, by a particle error distribution, which contains plenty of data points. Thus, they capture better the model behavior at expenses of a higher computational cost. As a result, they are considered as an alternative to the Kalman filtering techniques in the case of highly non-linear transition models.

Many approaches have been presented for AINS multisensor data fusion, but in few publications the results are field tested and evaluated using a ground truth. Beiter, 1998, states that it is possible to bound the position error growth rates to only a few meters per hour in a DVL/AINS without underwater absolute measurments. The authors propose the use of a 32-state Kalman filter, in which the dynamic system error propagation is modeled in real time, being the error state parameters estimated from the sensor data. Simulation results show that the model converges, but no real field data is shown.

Using absolute position fixes, Jourdan, 1997 presents a simple and improved USBL/AINS, it presents the results without ground truth, doing a comparison between DR, USBL and the output of the Kalman filter.

Ribas, 2012b presents the design of a delayed state information filter to estimate the vehicle pose from DR, DVL and USBL. The objective of this work is to evaluate the measurement delay integration

on the filter, but not the trajectory error using an USBL system. The behavior of the filter with and without delayed measurements is compared to the previously used EKF presented in Ridao, 2011 using a USBL aided reference trajectory with added delay.

Caiti, 2014, proposes an acoustic positioning system based on an USBL and four modems. The authors evaluate the system using punctual GPS ground truth at some instants of the trajectory. In Caiti et al., 2014 they integrate the acoustic positioning readings in an EKF and evaluate the estimated trajectory with a GPS ground truth. The used AUV has a USBL installed facing downwards, in such a way that while the vehicle navigates on surface it receives GPS and USBL measurements. With the same physical setup Di Corato, 2014 and Allotta, 2015 extend the USBL field tests with the application of an acoustic-based SLAM, without any prior information about the moored modems positions. Allotta, 2016 shows the implementation of an unscented Kalman filter, and a comparison with an EKF. It concludes that as the set of sensors is reduced the UKF provides more accurate estimations.

USBL systems have been used for many years, they have an easy deployment and an adequate precision for many marine tasks. As explained in section 2.4, an USBL system is composed by an hydrophone array, an attitude heading reference system (AHRS) and a global positioning system (GPS) in order to reference the relative USBL measurements to a world reference frame. In Sun, 2014 the precision of the USBL is evaluated using error ellipse theory, they assume that the USBL measurements follow a Gaussian distribution given by the random errors. It finally concludes that the overall positioning measurements considering USBL, GPS, AHRS do not follow a normal distribution due to the inevitable existence of system errors produced by sensor miscalibrations.

On that assumption, that the USBL observations have added non-Gaussian noise, Rigby, 2006 presents the fusion of USBL observations with DVL aided DR measurements using a particle filter. They use the AUV's GPS as a ground truth, being aware that the on board non-differential GPS measurements may contain errors of 5 meters approx.

1.5 Methodology

An iterative methodology has been used for the development of this project: any of the topics related with communications, measurement and position estimation have stared with a documentation period, about the state of the art and the used technologies. Then, a sequence based on design, implementation and testing of the different approaches has lead to an iterative cycle until all the objectives have been fulfilled.

The pipeline that has been followed, subject to some timing constraints, starts with a wide research on the state of the art on underwater robotics, acoustic technology, and the different methods used to establish communications and get absolute position measurements underwater. Besides, a familiarization with the used robot has been performed, in order to get fluent with the existing software architecture. All of this documentation has provided more insight on the subject and has lead to take better decisions on the design and implementation stages. However, since the documentation and familiarization was very extensive, it has been extended along the project, relaying on the scheduled milestones.

The first implementations to set the acoustic communications working, and linked the software architecture based on the Robot Operating System (ROS), have been tested in simulation and in an small pool. Next step has been to develop the positioning software and to design the hardware setup, as well as start thinking in any possible source of ground truth to evaluate the measurements obtained during field tests. The ground truth registration, with the current resources, has been a main concert through all the project.

Then, the first measurement tests started at the sea, followed by the filtering techniques testing, and a continuous loop of test and development of new solutions. Finally an approximate ground truth have been used for the validation of the system and a comparison between the performance of two filtering techniques has been performed.

Since field tests are very costly and time consuming, they require equipment preparation and installation, because of that they have been designed beforehand in order to prioritize the different tests.

The appendix section A contains the planning for the project development designed when the project started, and the real schedule that has been followed, the possible causes preventing the normal execution of the planning will be exposed.

Chapter 2

Background

This section exposes the theoretical background in which this project is based. It starts introducing underwater robotics in section 2.1, the particular problems and differences with other robotic fields and the different sensors and technologies used.

Then, a detailed presentation of the robotic system that has been used will be given, section 2.2, focusing on the sensorial payload and providing a description of its capabilities. Then, will be described which was the original setup before the implantation before the execution of this project. The software architecture will be also briefly introduced in order to provide the big picture of the system.

Afterwards, description about the basics of acoustic technology for underwater applications will be given, section 2.3, providing an overview of such technology and the variety of systems that exist for both communication and positioning. More specifically, will be provided more details about the device chosen to be integrated in the vehicle, the USBL, section 2.4.

Finally some concepts related with robot localization will be reviewed, section 2.5. Introducing two Kalman based estimation techniques, the extended Kalman filter (EKF) and the unscented Kalman filter (UKF).

2.1 Underwater robotics

Many technologies have been developed for communication and localization of mobile robots, but the solutions may differ a lot depending on the kind of environment where the robot performs. Most developments have been produced in human structured environments, technologies such as the GPS, WIFI or Bluetooth have become a build-in feature for almost any new electronic product, in the new era of the internet of things (IoT). In underwater environments the paradigm changes. Since electromagnetic signals do not propagate well underwater, the previously commented wireless technologies can not be used and other techniques have been developed.

Not only in communications, but also in image processing. Underwater, many general cutting edge computer vision algorithms do not work properly. In this medium, different type of image corruptions appear that complicates the task of feature extraction and matching between images. Some examples of image corruptions are the flickering produced by the reflection of sunlight from the dynamic sea surface to the sea bottom, the scattering and back-scattering effects produced by the reflection of the AUVs light onto suspended sea particles and, last but not the least, the lose of color richness caused by water absorption. Image corruptions produce blur and haze, even when it is close enough. For the reader interested in underwater image pre-processing please refer to Chao, 2010, Chiang, 2012, Galdran, 2015 and Burguera, 2016b for correction approaches to scattering, haze and color absorption.

Acoustic transmissions were presented as a promising solution for both technology issues, communication and localization. Sound speed in water is up to 4.3 times faster than in air, $c_{water} \approx 1500 m/s$[1].

[1] Lysanov, 2001, refer to section 2.3.1 for further details.

Therefore, instead of using electromagnetic waves, acoustic waves emerge as a convenient way for underwater communication. However, underwater acoustics have several challenges to overcome: multipath propagation, signal attenuation, low latency and low rates that may produce communication delays and transmission looses. Nevertheless, the low enough sound speed in water allows the measuring of transmission times, which can be used to get relative position estimates, section 2.3.

2.2 System

This section presents the basis of the robotic system, including the AUV, the ground station (GS), and the original physical setup and software architecture.

2.2.1 AUV

The USBL aided navigation has been integrated in the Turbot AUV owned by the University of the Balearic Islands (UIB). The Turbot AUV is based on an SparusII AUV unit, Carreras, 2013, designed and built by the Underwater Robotics Research Center (CIRS) of the University of Girona (UdG). And a sensor payload designed and built by the Systems, Vision & Robotics (SRV) group of the UIB.

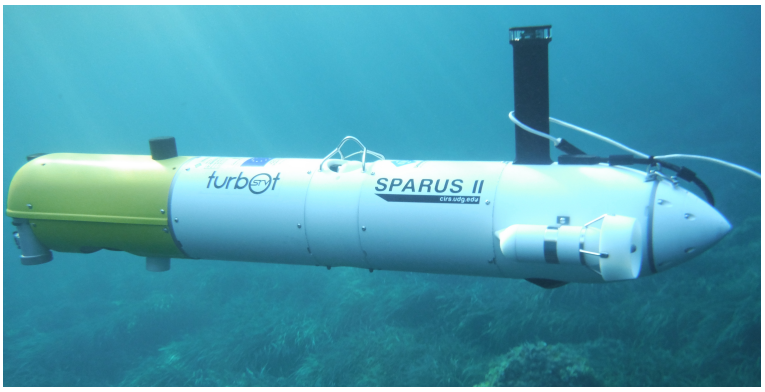

FIGURE 2.1: Turbot AUV

Length	1.6m
Hull diameter	230 mm
Max width	460 mm
Weight in air	52 Kg
Maximum depth	200 m
Energy	1.4 kWh Li-Ion batt.
Controlled DOFs	Surge, Heave, Heading
Max surge velocity	3-4 knots
Structure	modular aluminum and acetal hull
Software	Linux Ubuntu 16.04 and ROS Kinetic
Payload Interface	Ethernet, RS-232 / regulated 12V and 24V
Communications	WiFi, acoustic modem
Safety	Emergency primary batt., independent pinger tracking system, flasher light, USBL and acoustic modem.

TABLE 2.1: Turbot specifications

SparusII AUV, is a torpedo shaped lightweight hovering vehicle, with efficient hydrodynamics for long missions in shallow waters, and a software architecture based on the robot operating system ROS,

Quigley, 2009, named COLA2, Palomeras, 2012. It has three degrees of maneuverability, it can directly control heave, surge and heading, this is (x, z, ϕ). Two parallel and horizontal thrusters at the tail control have and heading, while one vertical thruster in the middle of the AUV, at the center of mass/buoyancy, controls the surge. Table 2.1 shows some of the technical specifications of the Turbot AUV.

Sensor	**Reference Name**
IMU + Compass	ADIS16488AMLZ
Pressure	Honeywell 19c
GPS	Adafruit Ultimate GPS Breakout
DVL	Teledyne ExplorerDVL Piston
Camera rig	AVT Manta G-283C
Modem	Evologics S2CR 18/34 Delrin

TABLE 2.2: Turbot navigation sensors

Turbot AUV has recently increased it's sensing capabilities. It has the usual proprioceptive sensors; an inertial measurement unit (IMU), a compass and a pressure sensor. Moreover, dead-reckoning from the proprioceptive sensors is aided with a Doppler velocity log (DVL), an acoustic device able to estimate linear velocities relative to the water column or using bottom tracking. Furthermore, the robot has an stereo rig from which visual odometry can be obtained, used for absolute positioning of the vehicle using visual SLAM, and to gather data for 2D or 3D reconstructions, Bonin-Font, 2015; Negre, 2016. A slightly tilted laser stripe projector is also mounted to obtain 3D reconstructions, as well as two 4320 lumen LED lights to work in low natural light conditions. There is also installed a Miniking imaging sonar, to perform obstacle avoidance, and a GPS to get absolute position fixes when the vehicle is at surface. It has also an acoustic modem used for communications and positioning, which has been set up in the context of this Thesis. More information about the Turbot AUV can be consulted in Massot, 2016. Additionally, specifications of all the sensors, table 2.2, can be found in the appendix B.

2.2.2 Previous setup

The previous working setup when performing a field test is displayed in figures 2.2 and 2.3. Communications were performed using a catamaran shaped antenna, connected to the AUV through a 10m Ethernet wire with an underwater SubConn connector. An omnidirectional antenna connected to the ground station computer. Both antennas established a WLAN network link.

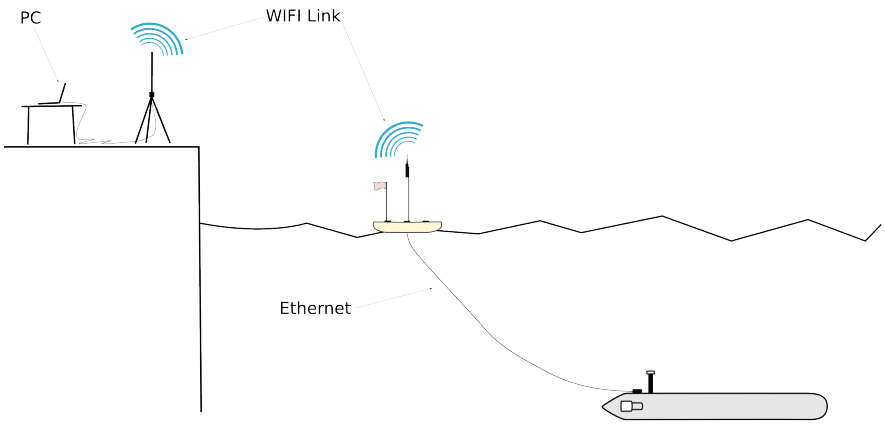

FIGURE 2.2: Original setup - Scheme

(A) Ground Station

(B) AUV with the catamaran shaped WLAN link tethered.

FIGURE 2.3: Original setup - Sea Trials

This setup had several limitations both in communication and localization. With respect to the localization issues: there were absolute position fixes only when performing on surface, GPS, and seafloor, visual SLAM. In the mid-water column transition, and even in seafloor situations when the images did not satisfy the SLAM requirements, the estimated position differed from the real one due to the drift caused by the pure odometric pose estimation. A feature rich sea bottom and a trajectory with many loop closings is required for a proper performance of the visual SLAM, Bonin-Font, 2015.

Regarding to communications, even though the WLAN has a wide bandwidth that allows to monitor the vehicle status, it has a limited operational range of $300m$. Moreover, the wired Ethernet connection with the catamaran-shaped antenna has some obvious limitations; it not only sets a limit for the operational depth, but also affects to the dynamics of the vehicle.

The robot's autonomous navigation can be supervised using a web interface, also developed in the SRV group. It consists in a javascript programmed web, linked to the robot software architecture, section 2.2.3, from which the robot status can be monitored and commands can be sent. Figure 2.4 shows an screen-shot of the interface, where a survey path has been set as a trajectory command, represented in green. The trajectory estimated by the AUV is represented in pink. Several commands can be sent to the AUV; emergency surface, disable thrusters, set lights on/off, start/stop recording, etc.

(A)

FIGURE 2.4: Robot missions interface

The AUV can also be remotely operated with a joy connected via Bluetooth to the ground station PC. As a safety measure the joy commands overwrite the autonomous navigation commands, in order to be able to take control of the robot if necessary. Joy commands consist in velocity references, but there is also a command to keep robot's position.

2.2.3 Software architecture

Robot architecture is based on the Robotic Operating System (ROS), Quigley, 2009, and has been programmed using C++ and Python languages. As shown in figure 2.5, all the software architecture is divided in three layers; navigation, safety and control. It is an extension of the COLA2 architecture provided with the SparusII AUV, Palomeras, 2012.

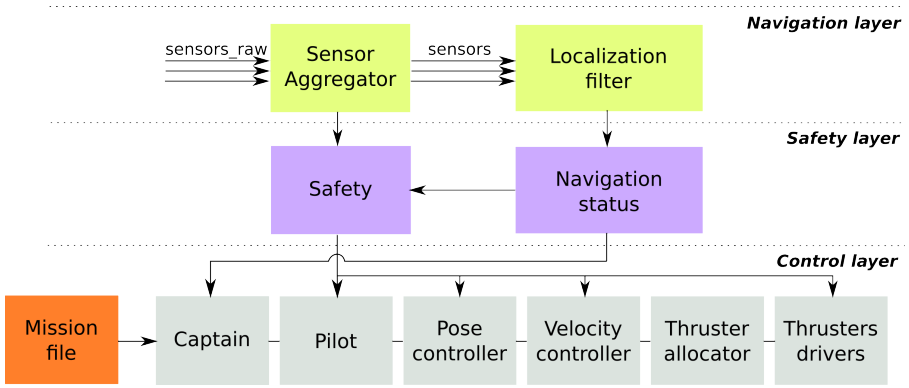

FIGURE 2.5: Software architecture

The navigation layer address all the sensor input management: raw measurements are directed to a node which centralizes and supervises the proper operation of all sensors, in case of any difficulty it sends an alarm to the safety layer. Furthermore, it checks some some sensorial conditions that are required in order to start the autonomous navigation. Before enabling the localization filter all the sensors are listened in order to see if they have been initialized correctly, and if they publish at the desired rate. The node sets the start position of the filter, based on the GPS. Then, the filter is enabled using a service and it starts estimating robot's pose. Sensor measurements can be sent then to the localization filter, that will produce an estimate of the current state of the robot.

The safety layer is constantly monitoring the navigation, it provides navigation feedback to the controller and is able to abort mission if an alarm is received, making the robot return to surface.

An other added feature of the web interface, is the possibility of creating the robot's missions directly in it, which allows to set several trajectory surveys based on way-points. A captain node reads the missions files and sequentially sends the way-points to a pilot node, which performs the local trajectory planning. One way-point is assumed to be achieved when the robot is at a threshold distance of it; for the trajectories to perform in this work a threshold of $2m$ will be used.

Only one core is used to run the ROS architecture, it is located at the AUV and shared with the ground station PC that runs the high level commands using the web app. In any case an SSH connection is established through terminal commands to modify and launch programs when needed.

2.3 Underwater Acoustics

2.3.1 Sound propagation

This section introduces underlying topics regarding sound propagation, to see the different inconveniences that may appear in shallow or in deep waters. Most of the introduced theory has been obtained from Lysanov, 2001, book about ocean acoustics. The authors state that the most characteristic feature of the oceanic medium is its inhomogeneous nature, which has an strong influence on the sound propagation. Two type of inhomogeneities exist; regular and random.

The sound velocity in sea water is not homogeneous, it lies between 1450 and $1550 m/s$. It has a regular inhomogeneity component that depends on the temperature, salinity and pressure. Expression 2.1 shows a relation to obtain an estimation of the sound speed $c[m/s]$, when the temperature $T[^\circ\mathrm{C}]$,

the salinity S in parts per thousand and the depth $z[m]$ are known. Besides, a random inhomogeneitiy component may be the cause of sound wave scattering, fluctuations and absorption.

$$c = 1449.2 + 4.6T - 0.055T^2 + 0.00029T^3 + (1.34 - 0.010T)(S - 35) + 0.016z \tag{2.1}$$

A sound velocity profile $c(z)$ found in shallow waters is represented in figure 2.6a. It is a common profile during summer-autumn seasons: when the top layers are well heated the sound speed increases. Figure 2.6b shows a ray diagram which represents the principal wavefront directions of the sound waves produced at z_1. Every reflection increases acoustic signal attenuation, shortening the operational range of the acoustic communication. Signal attenuation is caused by the combined effect of absorption and scattering. Sea bottom reflections cause significant signal absorption, whereas surface reflections cause scattering due to a rough ocean surface and the presence of air bubbles.

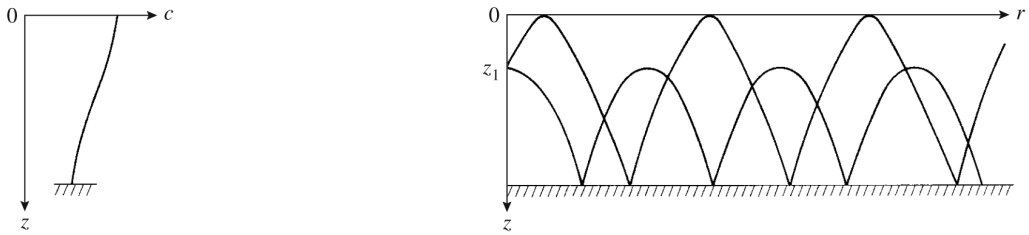

(A) Velocity profile $c(z)$. (B) Ray diagram.

FIGURE 2.6: Sound propagation in shallow waters.

In deep sea, high range transmissions are possible due to the existence of a minimum in the velocity profile, figure 2.7a. The minimum velocity, is produced by higher temperatures at the surface and higher pressures for large depths. When the minimum is sufficiently far from the sea bottom, part of the sound energy is trapped in an underwater sound channel, without any signal attenuation caused by bottom or surface reflections, figure 2.7b.

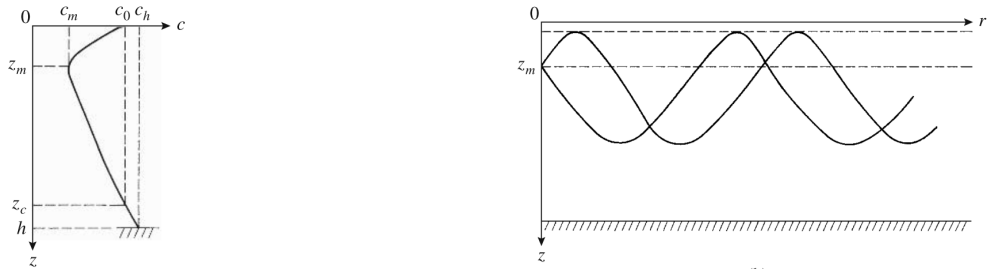

(A) Velocity profile $c(z)$. (B) Ray diagram.

FIGURE 2.7: Sound propagation in deep sea.

Large assemblages of small marine animals are another reason for signal attenuation, causing both scattering and absorption. Moreover, part of the acoustic energy is absorbed by the ocean and transformed into heat. Sea water viscosity is the main cause of the absorption of acoustic signals which frequencies lie in between 100 Hz and 100 kHz. Many other factors may affect to sound propagation: currents, internal waves and small-scale turbulence add noise effects over the velocity profiles, resulting in fluctuations on the intensity and phase of the sound waves.

2.3.2 Communication

Underwater acoustic (UWA) communications are a rapidly growing field in research due to the increasing needs of AUV underwater communications, as well as the energy dissipation of electromagnetic waves, section 2.1. Nowadays it is a mature technology, but further development is done since it is the most used technology for wireless underwater communication and positioning, having lots of performance issues to improve. The low bandwidth, high transmission loses, multipath propagation, high latency and Doppler spread are the main drawbacks of this technology. They keep researchers working on further improvement and development of new technologies.

Many research and commercial acoustic modems have been developed to allow slow and stable high range communications, even for environments cluttered of sound propagation inhomogeneities. An acoustic modem is usually based on the scheme presented in figure 2.8. It consists on a digital stack based on an analog-to-digital converter, a digital-to-analog converter, a digital signal processor and a field-programmable gate array. An hydrophone is used to receive acoustic signals, and a loudspeaker to emit them.

Recalling that a transponder is a device that emits a particular signal in response to an interrogating received signal, and that a transducer is a device that converts one form of energy into another. We will refer to either hydrophones and loudspeakers when we talk about transducers.

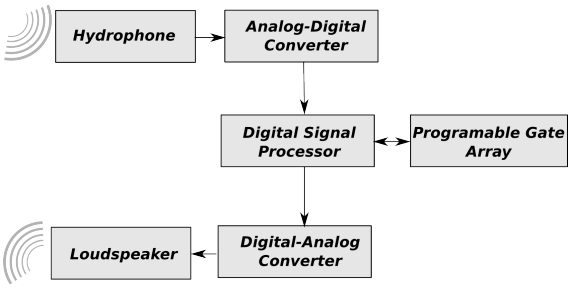

FIGURE 2.8: Acoustic modem scheme.

2.3.3 Positioning

In contrast with electromagnetic communications, taking advantage of the precision of the actual clocks and the sufficient sound speed in water, underwater positioning can be obtained from the time of flight (TOF) of an acoustic signal, that is the time that takes an acoustic signal to travel from one transducer to another. Having an estimation of the sound speed in water, c_w, a distance measure d can be obtained from the TOF, equation 2.2.

$$d = c_w \cdot tof \tag{2.2}$$

Each transducer provides a range measurement that can be used as a distance condition in form of the spherical equation 2.3. Where (x_0, y_0, z_0) and (x, y, z) represent the known and the not known transducer position respectively. Hence, an acoustic positioning system needs at least 3 transducers located at known positions, in order to determine the position of a fourth transducer. In other words, to determine a 3D position three points have to be located in the space, as well as the distances to such points, there will be three spherical equations which determine a three dimensional point.

$$d^2 = (x - x_0)^2 + (y - y_0)^2 + (z - z_0)^2 \tag{2.3}$$

Measurement uncertainty is usually reduced by using more than three transducers. In this case, a position estimation might be obtained using different transducer triads estimations, or directly by solving the overdetermined problem using, for example, *Least Squares*.

Configurations The most usual acoustic positioning configurations are the long baseline (LBL) and the ultra-short baseline (USBL), represented in figures 2.9 and 2.10. The baseline refers to the distance between transducers.

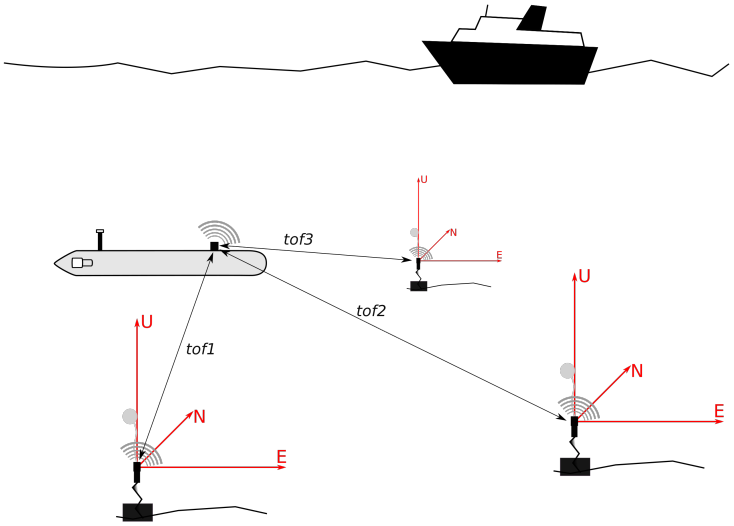

FIGURE 2.9: Long baseline - LBL

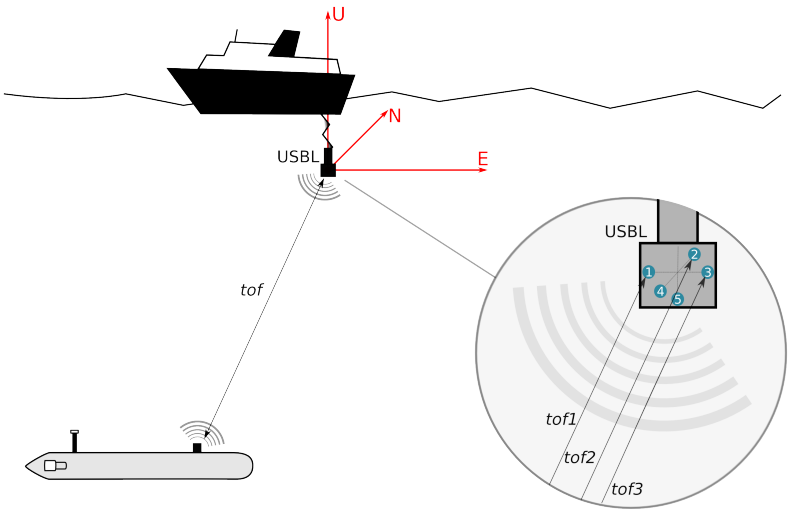

FIGURE 2.10: Ultra-short baseline - USBL

The LBL system requires the installation of at least three separated transponders at known positions, in order to triangulate the modem position. The modem constantly sends signals to the transponders, which is replied by each one of the transponders, and a position estimate is computed, from each TOF.

Since the uncertainty over the transponders is directly related on the uncertainty over the position estimate, it is rather important to perform an accurate installation. The usual installation fixes the transponders at the sea bottom in disperse positions. A calibration is performed then to determine the transponder's locations using a modem and a GPS from a ship, usually performing some large trajectories over the working area.

USBL systems require to install only one static device, in which several transducers are contained. Figure 2.11b shows the setup of the build-in transducers. The USBL pose can be precisely known using an on board GPS and an attitude heading reference system AHRS. Occasional calibration for the inertial sensor misalignment could be required.

(A) Reference frame (B) Transducers array (top view)

FIGURE 2.11: USBL device

The difference between both systems is basically related on the setup easiness, and on the measurement precision and accuracy. The USBL is a ready-to-go solution, whereas the LBL has a more arduous installation and harvesting. Regarding to the accuracy and precision, the LBL system is clearly the best solution: the higher baseline induce less bearing and elevation errors when computing the target position, recall the spherical representation of the expression 2.3.

The interesting point of the acoustic positioning systems is that they use the data transmission to compute the target position without having to switch between communication or location modes.

It computes a position estimation from the round-trip of an acoustic signal, figure 2.12. It starts in the USBL device, travels to the modem and then the latter creates a response that returns to the USBL. A *tof* is measured for every hydrophone, and then a position estimation is computed for each one of the considered triads.

2.4 USBL device

In order to estimate the vehicle's position the devices used for communication will be the following: a modem in the AUV, and an Ultra-short baseline USBL connected to the ground station. Both devices are from EvoLogics GmbH[2]. It's physical layer implements the Sweep-Spread Carrier (S2C) protocol, Kebkal, 2012. It evaluates the underwater acoustic channel parameters, detects the data packets and modulates and demodulates the acoustic signals. This technology is very convenient when dynamic environment parameters or multipath signal propagation may exist. It has implemented adaptive algorithms in order to estimate current channel parameters and get the highest bitrate possible in both, deep and shallow waters. Furthermore, S2C provide full duplex bidirectional data transmissions.

The model selected, S2CR 18/34, has data transmission up to 13.9 kbits/s with an operating range of 3500m and a maximum deployment depth of 200m, limited by it's Delrin housing. The detailed specifications are shown in the appendix B.1. It has integrated an AHRS (Altitude Heading Reference

[2]EvoLogics GmbH. https://www.evologics.de/

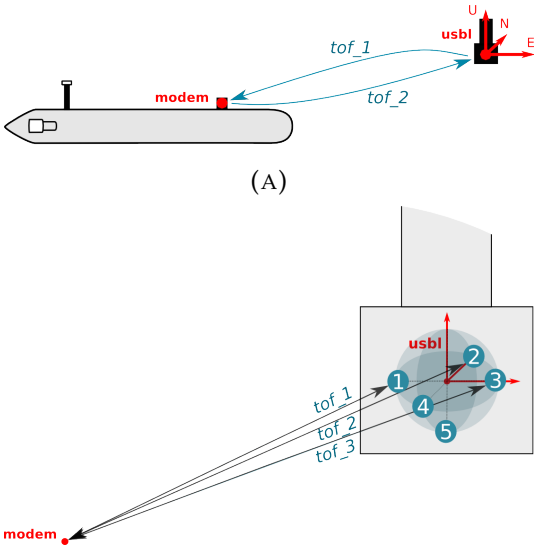

FIGURE 2.12: Acoustic wave time of flight

System) that provides the USBL orientation with respect to an standard ENU (East North Up) reference frame. Then, relative positions can be obtained from the communications between the USBL and modem devices, referenced to the USBL unit reference frame in ENU coordinates.

It computes a position estimation from the round-trip of an acoustic signal, figure 2.12. It starts in the USBL device, travels to the modem and the later creates a response that returns to the USBL. Having a total of five hydrophones, five TOF can be measured. It considers up to six triads in order to get six position estimations to help improving measurement precision, figure 2.13.

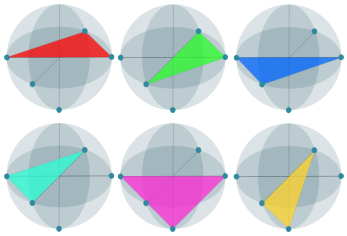

FIGURE 2.13: Six considered triads of the Evologics S2CR 18/34 USBL to estimate a position; 1-2-3, 4-3-2, 3-4-1, 4-2-1, 1-5-3 and 2-5-4.

2.5 Localization

Autonomous navigation requires improved localization modules to withstand the increasing demand on mission duration and higher accuracy. Nowadays, most AUVs still rely on dead-reckoning systems (DVL, visual odometers, inertial sensors) which are subject to accumulative drift. Absolute-sensing devices, such as GPS, pressure sensors and LBL or USBL Willemenot, 2009 can reduce the accumulated error and correct the position of the robot if handled properly.

Estimation filters are required to fuse the measurements provided by an heterogeneous set of sensors. Kalman based techniques assume a Gaussian distribution of the state variable uncertainty, allowing an efficient computation with robust performance when the Gaussian assumption is satisfied. In contrast, other techniques based in particle filters, or Montecarlo methods, might be more processor and memory consuming but guarantee a good performance without a Gaussian error distribution requirement.

This section presents the standard implementation of the extended Kalman filter (EKF) and the unscented Kalman filter (UKF), which will be used further in the document.

2.5.1 Extended Kalman Filter - EKF

Even though the Extended Kalman Filter (EKF) is a well known algorithm, we present here the basic ideas. It defines the robot system state x_k and the robot's system measurements z_k, at time k, as the result of the following dynamic processes

$$x_k = f(x_{k-1}) + w_{k-1} \tag{2.4}$$
$$z_k = h(x_k) + v_{k-1} \tag{2.5}$$

being f a nonlinear state transition function, and h a nonlinear sensor model. Both processes have added Gaussian white noise, w_{k-1} and v_{k-1}.

The filter performs a prediction and an update step per iteration. The prediction step projects the actual state and covariance by using the nonlinear state transition function, equations 2.6 and 2.7.

$$\hat{x_k} = f(x_{k-1}) \tag{2.6}$$
$$\hat{P_k} = FP_{k-1}F^\top + Q \tag{2.7}$$

The estimated error covariance P, is projected from the the Jacobian of f, F, and perturbed with the process noise covariance Q. The correction step works as follows.

$$K = \hat{P_k}H^\top(H\hat{P_k}H^\top + R)^{-1} \tag{2.8}$$
$$x_k = \hat{x_k} + K(z - H\hat{x_k}) \tag{2.9}$$
$$P_k = (I - KH)\hat{P_k}(I - KH)^\top + KRK^\top \tag{2.10}$$

The Kalman gain K is obtained using: the jacobian of the nonlinear sensor model, or observation matrix H, the measurement covariance R, and the predicted state covariance $\hat{P_k}$, equation 2.8. In equation 2.9 the Kalman gain is used as a weight that multiplies to the difference seen between the prediction and the measurement -the so called innovation factor-, which is the term that is added to the predicted state in order to produce the state estimation. Then, in equation 2.10 the new covariance estimation is produced.

It recursively provides the optimal minimum mean-squared error estimate for the state assuming that the previous estimate and the current observation are Gaussian random variables, due to the Gaussian white noise assumption of the models.

As shown, EKF deals with nonlinear models by linearizing until the first Taylor expansion, a simplification that may introduce important errors in the posterior mean and covariance, leading to sub-optimal or divergent results.

2.5.2 Unscented Kalman Filter - UKF

The Unscented Kalman Filter (UKF) avoids the propagation of a Gaussian random variable through first order linearization of the process dynamics, it addresses the problem in a deterministic manner. In the same way as in the EKF, this filter also assumes a Gaussian state distribution, but it represents the distribution using a set of points -sigma points- that have been chosen carefully. It tries to capture the posterior mean and covariance up to the third Taylor expansion, having smaller approximation errors than the EKF.

The unscented transformation is a method that is used to obtain statistics from a random variables, the nonlinear transformations are not done directly over the random distribution but over the statistics that represent it. Having the nonlinear transformation $y = g(x)$, where the state variable x has mean $\bar{x}$, covariance P_x and dimension L. A matrix χ can be formed with $2L + 1$ vectors χ_i ,

$$\chi_0 = \bar{x} \tag{2.11}$$

$$\chi_i = \bar{x} + \left(\sqrt[2]{(L+\lambda) P_x}\right)_i \qquad i = 1, ..., L \tag{2.12}$$

$$\chi_i = \bar{x} - \left(\sqrt[2]{(L+\lambda) P_x}\right)_{i-L} \qquad i = L+1, ..., 2L \tag{2.13}$$

where $\lambda = \alpha^2 (L + \kappa) - L$ is a scaling parameter. The spread of the sigma points around the mean is determined by α, and κ is a secondary scaling factor usually set to zero, used for "fine tune" of higher orders of approximation. The statistic vectors are propagated through the nonlinear expression $\phi_i = g(\chi_i)$ for $i = 0, ..., 2L$, and the transformed mean and covariance are given by,

$$\bar{y} = \sum_{i=0}^{2L} W_i^{(m)} \phi_i \tag{2.14}$$

$$P_y = \sum_{i=0}^{2L} W_i^{(c)} (\phi_i - \bar{y}) (\phi_i - \bar{y})^\top \tag{2.15}$$

$$\tag{2.16}$$

Being W_i the correspondent weights associated to each sigma point,

$$W_0^{(m)} = \frac{\lambda}{L+\lambda} \tag{2.17}$$

$$W_0^{(c)} = \frac{\lambda}{L+\lambda} + \left(1 - \alpha^2 + \beta\right) \tag{2.18}$$

$$W_i^{(m)} = W_i^{(c)} = \frac{1}{2(L+\lambda)} \qquad i = 1, ..., 2L \tag{2.19}$$

where β integrates the prior knowledge about the distribution, $\beta = 2$ is considered to be optimal for Gaussian distributions.

It results in approximations accurate up to a third order for Gaussian inputs, for other inputs the approximations will be accurate at least up to a second order. The accuracy of third and higher orders will be determined by the tuning of the internal parameters α, κ and β.

The UKF uses the unscented transformation iteratively to make the predictions of the states and observations by augmenting the state vector with the process and observation noise, in that way it avoids the use of Jacobians or Hessians obtaining high order approximations.

Chapter 3

USBL Integration

This chapter describes the USBL system integration developed in this work. The new physical setup is presented in section 3.1. The main ideas about the comunications and positioning implementation are presented then in the sections 3.2 and 3.3. Furthermore, the main structure modified software architecture is exposed in section 3.4. After the integration of the system proposed in this chapter, the AUV have been able to integrate absolute position measurements with the rest of the sensor set to produce accurate pose estimations. Besides, it has been able navigate and follow commands using only acoustic communication.

3.1 USBL system setup

The new system consists in two parts, the AUV and the ground station (GS). The GS has an associated PC connected through Ethernet to the USBL system, which is formed by an USBL device attached to a GPS intelligent buoy (GIB) that will provide the USBL absolute position.

The USBL system is outlined in figure 3.3b. The USBL is connected to the ground station PC through Ethernet connection, it sends the relative positions of the modem with respect to the USBL reference frame. Accordingly to the Evologics manual, the setup has to satisfy some requirements to work with minimum guarantees, even in shallow waters the USBL device has to be surrounded by at least 2m of water to avid possible multipath due to surface o walls closeness. Therefore, the buoy is moored as far as possible, usually $30m$ distance from the ground, at $2 - 3m$ depth, figure 3.1.

FIGURE 3.1: USBL system

The GIB system consists in a Raspberry Pi 3 Model B (RP3) [1] with an Ultimate GPS Breakout v3 module, figure 3.2b. The USBL device is connected by LAN to the GS Ethernet switch, and is powered using a DC power source of 24v. Furthermore, the RP3 is connected to the GS switch using another Ethernet connection and is powered with the same DC power source. Since the RP3 requires a 5v input, a DC-DC buck converter has been integrated to provide 5v from the supplied 24v. In order to avoid the overheating of the RP3 after several hours at the sun, some reflectors have been added to the continent box, as well as a 5v fan. The GPS box connections with the Ethernet wire are done using a Buccaneer[2] connector, in order to be waterproofed. The unions between box, buoy, pole and USBL have been done rigid in order to have an static transformation between GPS and USBL, figure 3.2a.

[1] Raspberry Pi 3 Model B. https://www.raspberrypi.org/products/raspberry-pi-3-model-b/
[2] Buccaneer connector. http://www.bulgin.com/products/circular-power-connectors.html

(A) USBL fixation to buoy pole.

(B) Buoy GPS box.

FIGURE 3.2

In this new setup, the robot manages all the navigation, safety and control, whereas the GS is used to produce an USBL position estimate and to monitor the robot when it is required.

3.2 Communication

The communication between GS and vehicle has been designed to have surface and underwater modes, represented in figure 3.3. In surface, the WLAN connection is established, providing a high transmission speed. While in underwater mode the communications will be minimal using the USBL acoustic communication system.

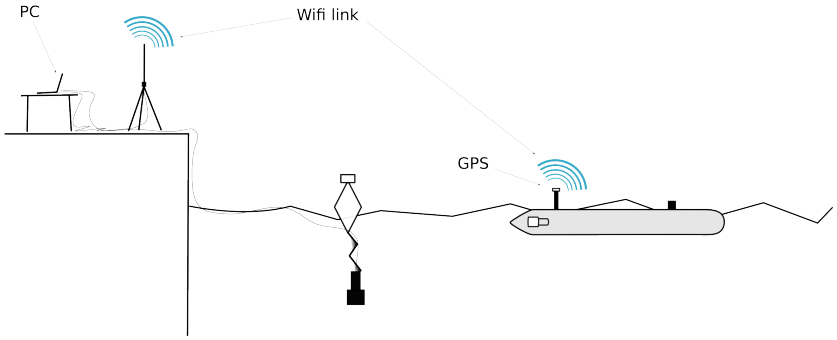

(A) Surface mode.

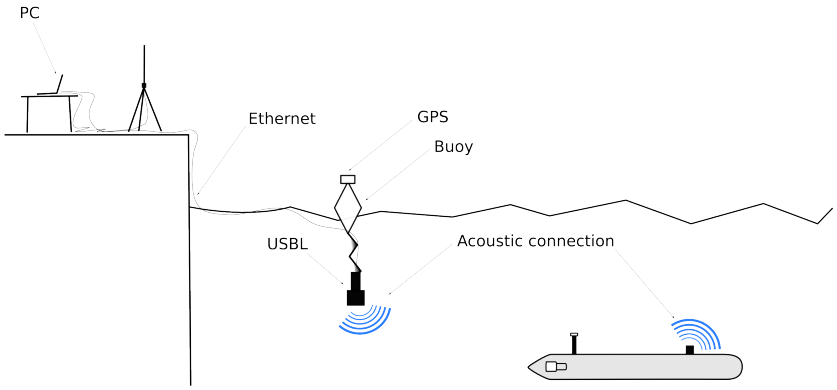

(B) Underwater mode.

FIGURE 3.3: New setup working modes.

The only changes on he AUV with respect to the original setup is that the catamaran shaped buoy is no longer needed and that the modem can be used instead.

3.2.1 Multimaster network

Having a software architecture based on ROS in both sides, all the information could be shared between both parts by using only one core, a ROS master. Since the acoustic communication bandwidth is very limited, GS and AUV can not share a ROS Master, neither a ROS Parameter Server. In the case of having the vehicle underwater, the slave would crash due to the lose of a proper WLAN link with the master.

Designing an strategy of communication between cores we are able to launch the architecture with separate cores in both sides. The ROS package multimaster_fkie[3] permits to use a multimaster network when Ethernet connection is available, then, it enables communications between both ROS Masters when a WLAN connection is available, that's when the AUV is in surface mode. In underwater mode communication between cores is performed using acoustics, section 2.3.2.

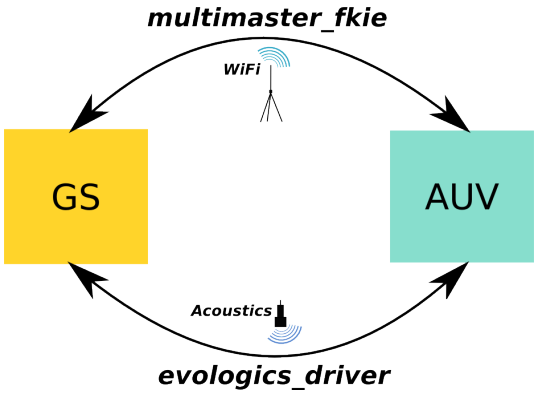

FIGURE 3.4: Multimaster approach.

In surface mode the supervision of the vehicle will be complete, all topics will be monitored in the GS. In underwater mode, due to the bit rate limitation, the available information of the AUV state in the GS will be minimal. In order to guarantee a correct supervision the navigation status will be periodically sent to the GS, as well as any control or safety service from GS to AUV.

3.2.2 Underwater mode

The installed USBL and modem devices already have a built-in acoustic communication protocol based on S2C, 2.4, controlled using string commands, in the case of the modem through serial connection, in the case of the USBL via Ethernet.

As stated in section 2.2.3, our software environment is based on ROS. Thus, in order to link the devices with the ROS architecture, a communication layer has been created able to transform ROS messages from the selected topics and services into string commands to be send acoustically. Likewise, it is able to receive messages acoustically through string commands and convert them into ROS messages to be advertised in their respective topics.

Then, three stages have been considered in the communication layer when the vehicle is in underwater mode to convert acoustic signals into ROS messages and vice versa; the communication device electronics (Signal converter and processor), which converts between acoustics and strings, a device driver to transform between strings to a general ROS message type, and a coding/decoding tool to compose between a general ROS message type and the specific types of ROS messages advertised.

Device electronics Some settings have to be configured beforehand in the device electronics of the communication device. Every device have to be associated to a different acoustic address, as well as a network IP in the case of the devices connected through LAN. Some other settings have to be set, but all

[3]ROS package multimaster_fkie. http://wiki.ros.org/multimaster_fkie

of them can be set when the device driver starts, that is the case of the source level for the output signals and the gain level for the input.

Device driver The driver has the purpose of being an interface for translating ROS topics and services into device commands that will be sent through serial or TCP ports. The *evologics_ros*[4] ROS package, based on the *evologics_driver*[5] of the Heriot-Watt University is able to produce string commands used to adjust internal device parameters, as well as to send and receive acoustic messages. It uses a general message type composed by some communication parameters and a data field of string format, called payload. For message reception, the driver is able to read a received string that contains a serialized message. Then a general ROS type message is build, being the received information stored in a string data field of the message. The message is advertised in a topic which contains all the incoming acoustic messages, which is subscribed by the coding/decoding node. For outgoing messages the procedure is the same but in the opposite direction, the driver is subscribed to a general ROS message topic used for outgoing messages, when a message is advertised the driver builds an string command which contains the string data field of the general message and it is send through serial or TCP connection depending on the used device.

Coding/decoding Since the information to be transmitted, topics and services, are contained in messages with different format, a general method to convert any type of message to the general message type is needed, an acoustic parser. Two different approaches have been developed to serialize specific ROS messages into an string to be send to the device driver inside a general ROS message type and vice versa. The type of messages used for the acoustic communications can have a maximum size of 64 bytes, so it is the limit for the string size.

The first approach, so called *acoustic_link*[6] is based on building the data field of the general message type with an specific structure tailored for each type of message. Designed with specific descriptions for parsing the messages of each one of the topics or services used.

A second approach using *rosserial*[7] package, is proposed as a promising solution to serialize any type of topic or service. After several modifications, the *rosserial_server*[8] package is able to listen any of the topics or services listed in a given parameter file and serialize each of the messages to put them in a string data field of a general message that will be read by the device driver. The inverse operation would be to advertise the listed topics of a parameter file, listen for incoming general messages and deserialize the string data field to create the specific messages that will be advertised by their respective topics.

Both implementations have their pros and cons, in the case of the *acoustic_link*, the node has to be tailored specifying callback and parsing functions for every type of message or service that will be used. Then, if new communications are needed, the node should be modified. This can be a tedious task if the robot architecture is usually changing and one might want to have a more general method in which indicate the desired communications by only editing a parameter file. The main reason against using *rosserial_server* is that the whareas the serialization is automatized for any new type of message, it's internal serializing functions provide longer strings that may lead to an overweighted message.

[4] evologics_ros package. https://github.com/srv/evologics_ros
[5] evologics_driver package. https://github.com/oceansystemslab/evologics_driver
[6] acoustic_link package. https://github.com/srv/acoustic_link
[7] rosserial package. https://github.com/ros-drivers/rosserial.git
[8] rosserial_server package. https://github.com/srv/rosserial/tree/indigo-devel/rosserial_server

3.3 Localization

This section focuses in two sides, the positioning measurement given by the USBL system and the integration of the measurement in the filter. It will be not only shown how the measurement is obtained, but also the approach that has been followed to process the measurement and insert it in the position estimation filter. The positioning algorithm pipeline is as follows. First, a relative position measurement is produced by the USBL, it is transformed to world coordinates using the GPS position given by the RP3 and is then sent to the AUV acoustically. When the measurement arrives to the AUV it incorporates a delay that depends on the communication distance, produced by the communication latency. Hence, the delayed measurement is updated using the the change of position during the delayed time estimated by the odometric sensors. At this stage an outlier rejection procedure is applied in order to get rid of bad data quality the different noise sources that may appear, refer to section 2.3. Finally, it is important to mention that the measurement degree of belief, the associated covariance, is propagated when a frame transformation by using linear error propagation.

3.3.1 Measurement

The algorithm starts when a relative measurement is received from the USBL in the GS. It provides the transformation between USBL and modem attached to the AUV, relative to the USBL frame. After some transformations it is sent to the AUV to be integrated in the positioning filter. The USBL measurement is obtained from the TOF as follows:

1. The USBL sends a ping to the modem.
2. The modem answers.
3. The USBL receives the response, produce the measurement, transforms and send it to the AUV.
4. The modem receives a delayed measurement in NED origin coordinates.

Looking at the figures 3.5 we can reason the following. Since the measurement is obtained from the time of flight of the acoustics signals as $tof = tof_1 + tof_2$, and assuming that the USBL is anchored and the response time of both can be neglected, $tof_1 = tof_2$. Hence, t_2 can be considered as the measurement time.

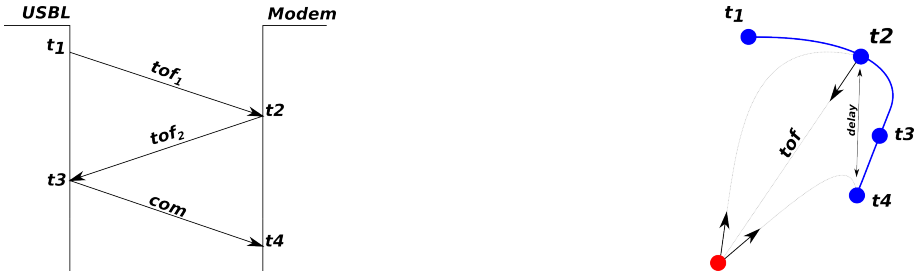

(A) (B)

FIGURE 3.5: USBL measurement TOF and delay. Where $t_{measurement} = t_2$ is the time in which the modem listens the query and answers

The relative measurement is transformed to the NED origin reference frame at t_3, and then it is sent acoustically to the robot. The measurement delay will be given by $d = t_4 - t_2$, $d = t_{actual} - t_{measurement}$, used to estimate the movement produced by the AUV since the measurement was taken. Having a sound speed in water around $1500m/s$ and an USBL operational range of $3500m$, since an acoustic signal has to be produced several times between USBL and modem, the measurement delay can be of the order of seconds, $d_max = 4.7s$. After the update of the measure it will be uesd by the localization filter.

Transform In the AUV architecture, the vehicle pose is given relative to a reference frame called NED origin, set at the navigation initialization following a North-East-Down convention. Consequently, modem positions seen from the USBL have to be given in the same reference frame.

The transformation between the NED origin and the USBL unit will be given by the GPS fixed rigidly to the USBL. Based on figure 3.6, equation 3.1 shows the desired transformation, where T_{ned}^{gps} is given by the GPS and T_{gps}^{usbl} is static and known. Reference frames are represented in figure 3.6.

$$T_{ned}^{modem} = T_{ned}^{gps} \cdot T_{gps}^{usbl} \cdot T_{usbl}^{modem}, \tag{3.1}$$

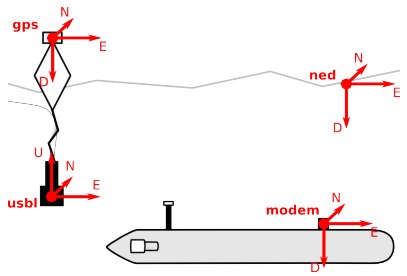

FIGURE 3.6: USBL positioning reference frames

Update The idea for the USBL delayed measurement update is represented in figure 3.7. It is very simple, when the robot receive a delayed USBL measurement $P(t_a)$ it looks in the memory which was its pose given by the odometric sensors at the USBL measurement time $P'(t_a)$, then it computes the odometry transformation from the measurement time to current time $T_{P'(t_a)}^{P'(t_b)}$, namely *delta_odom* in the figure, as the last measured trajectory offset. The updated USBL measurement $P(t_b)$ will be obtained by adding the odometry variation to the delayed measurement, as an offset correction.

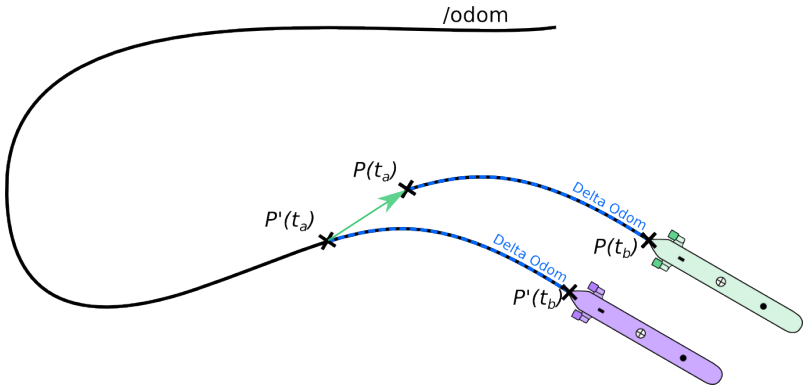

FIGURE 3.7: USBL position update

Since the USBL measurement only corrects position, we assume that the orientation is given by the old odometry $P'(t_a)$. This temporal transformation is shown in equation 3.2, where $\Delta odom$ will be based on a continuous odometric estimation given by the localization filter.

$$T_{ned}^{P(t_b)} = T_{ned}^{P(t_a)} \cdot \Delta odom = T_{ned}^{P(t_a)} \cdot T_{P'(t_a)}^{P'(t_b)} \tag{3.2}$$

Outliers rejection Many acoustic measurements come from noisy observations when the robot performs in a real, harsh and unstructured environment and may deteriorate the position estimation performance, refer to section 2.3. Also, after testing the used USBL device has not been found a direct correlation between the USBL measurement quality indicators provided (signal strength, integrity and

accuracy) with respect to the sensor error in order to qualify the measurement. Then, a simple strategy to filter outliers has been implemented. It consists in a threshold distance for the difference between the movement measured by the USBL during the last two samples received, and the movement estimated by the odometry filter during the same period.

Degree of belief Before integrating the updated measurement in the localization filter, we need to know which has to be the degree of belief that the filter has to have for the measurements. In other words, since we are working in a probabilistic frame, each estimated variable has to have an associated variance that indicates the measurement uncertainty.

The USBL device provides a confidence value associated to the measurements that is supposed to be the standard deviation of the position. However, it has been observed that the confidence measure is not very well correlated to the dispersion obtained. Either way, the experiments, section 4.1, have provided the precision of the device from which a measurement covariance can be set.

All the reference frame transformations consider their respective covariance propagation. The delayed measurement covariance that is sent to the robot is the propagation of the GPS and USBL uncertainties. This uncertainty propagation is done through linear error propagation using the operations provided by the ROS package mrpt-ros-pkg[9] for pose transformations.

3.3.2 Filter

The localization filter has been changed from the original EKF implemented in the COLA2 architecture, reviewed in 2.2.3, in order to ease the integration of a second absolute position measure. Now the implementation will be based on the EKF and UKF provided by the ROS package robot_localization[10], evaluated in Moore, 2014, 2016. Both EKF and UKF have been detailed in the section 2.5, and will be tested in the chapter 4.

After the measurement has been processed it may be introduced in the localization filter. The position estimation from the sensor measurements is given by two parallel filters. One filter is fed with all the dead-reckoning (DR) sensors (IMU, compass, DVL, visual odometry (VO) and depth) and provides a continuous odometry output. In contrast, the second filter integrates additionally the absolute positioning sensors, (GPS and USBL). Since the GPS and the USBL measurements consist in absolute corrections, the output of the second filter will be discontinuous. The Pressure sensor has been considered as relative due too its high precision and update rate. As we will see in the experiment sections, chapter 4, the smoothness of the output of the second filter will depend on the degree of belief that we assign to the absolute positioning measurements.

The continuous odometry estimation of the first filter will produce a precise estimation subject to drift for medium-large trajectories. However, it will produce very accurate for short term estimation, order of seconds. It is a continuous output estimation with a low noise rate, due to it does not have a mechanism to reset the accumulated error, the trajectory drift grows unbounded. This short term accurate position is important for different proposes, one of them is detailed in section 3.3.1, it helps to update delayed position measurements, using the estimation of a short term movement.

In contrast, the estimation for the second filter, which has absolute position measures, has higher noise rates. Nevertheless a great advantages that it has is that the noise is bounded. Summarizing, for short term estimations is better to use the output of the first filter, the output of the second will be used for long term. One of the topics that are supposed to be answered in this work is at which moment the absolute position given by the USBL integration provides better accuracy than the DVL aided DR estimation.

[9] mrpt-ros-pkg for pose transformations. https://github.com/mrpt-ros-pkg
[10] robot_localization. http://wiki.ros.org/robot_localization

3.4 ROS Implementation

This section provides the technical details about the implemented acoustic USBL positioning system presented in previous sections. All the implementation is synthesized in the schemes shown in the figures 3.8 and 3.9, they present the structure of nodes and topics used to generate a pose estimation with the USBL position measurement. All has been implemented using ROS and built in the software architecture presented in section 2.2.3.

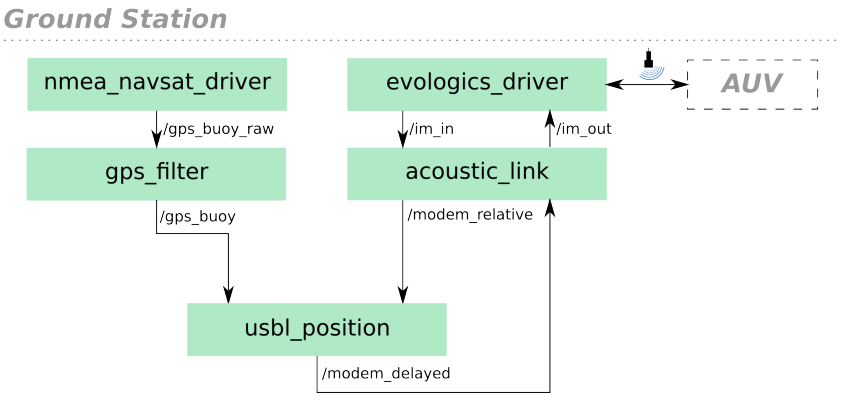

FIGURE 3.8: USBL measurement implementation in the ground station

The first one shows the software architecture of the ground station (GS). As stated in section 3.3 the GS generates a measurement that can be represented as the transformation T_{usbl}^{modem}, it is the modem position relative to the USBL reference frame. This measurement is provided by the USBL driver, namely *evologics_ros*[11]. At a first stage the measurement is carried by a generic message type and then introduced in the *acoustic_link*[12] node which has the objective of coding and decoding general messages to specific ones.

The GS also generates GPS measurements of the buoy location using the *nmea_navsat_driver*[13] package. The measurements are then filtered by computing the median of the last t seconds in a *gps_filter* node, assuming that the buoy is fixed a long period of time can be set to perform the mean.

Both measurements are then fed into the *usbl_position*, node contained in the developed *usbl_position*[14] which performs the required transformations to set the modem position referenced in NED origin coordinates, remember section 3.3.1. Finally the transformed position goes back to the communication nodes to be sent to the AUV.

The AUV part of the USBL positioning architecture work as follows. The received measurement is produced in the communication nodes, each acoustic message received by the modem is converted in a general message type by a second instance of the *evologics_ros* USBL driver and then transferred to the *acoustic_link* coding/decoding node of the AUV to build it in the correct message type. Since the acoustic measurement arrives to the AUV with up to some seconds of time delay, the *usbl_projection* node uses an estimation of the vehicle movement to update it, section 3.3.1.

Based on the ROS REP105 two filters are implemented in order to obtain two types of estimations. REP105 specifies a convention about the coordinate frames to use, the pose of the *base_link*, located at the robot, will move with continuity with respect to the *odom* frame, but not with respect to the *map* frame. Both are given in world coordinates, but the former is given by continuous odometric sensors, and the later also includes absolute positions that may produce discrete jumps.

In this implementation a pose estimation is performed in a filter using continuous data with respect to the *odom* frame, and another is also performed using all the sensors, including the USBL and the GPS,

[11] USBL ROS driver **evologics_ros**. https://github.com/srv/evologics_ros
[12] ROS message coding **acoustic_link**. https://github.com/srv/acoustic_link
[13] GPS ROS driver **nmea_navsat_driver**. https://github.com/srv/nmea_gps_driver
[14] USBL positioning system **usbl_position** package. https://github.com/srv/usbl_position

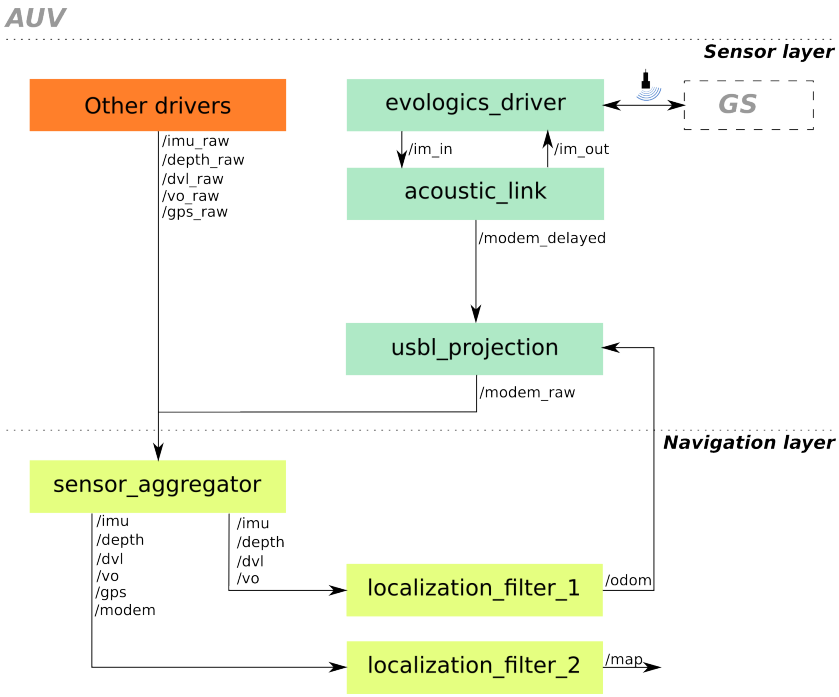

FIGURE 3.9: USBL measurement implementation in the AUV

to produce the long term estimation. The pose transformation between the output of the former and the latter will be the position of the *odom* frame with respect to the *map* frame. Note that the continuous estimation of the first filter is used as a movement estimation to update the USBL measurements since for short term odometry estimation is more precise than absolute estimation.

Odom Filter															
	x	**y**	**z**	**roll**	**pitch**	**yaw**	**vx**	**vy**	**vz**	**vroll**	**vpitch**	**vyaw**	**ax**	**ay**	**az**
IMU				X	X	X				X	X	X			
DVL							X	X	X						
VO							X	X	X	X	X	X			
Depth			X												

TABLE 3.1: Odom filter inputs

The *robot_localization*[15] package has been used for the estimation filters. One of the most important advantages that the package offers is that it allows pose estimation in 3D spaces using an unlimited number of sensors. But it does not end here, if a sensor is added or removed only a parameter file has to be edited. It is also flexible to the type of message received, and can be selected which information of the sensor messages should be inserted in the filter. It provides a more modular and standardized solution, than the previous approach.

Finally comment that the transformation and the update of the delayed measurement is done in two different nodes of the *usbl_position* ROS package to save acoustic transmission bandwidth. The GPS measurement needed to transform the USBL measurement is produced at the ground station, and the odometry obtained from the estimation filter needed to update the delayed measurement is produced in the robot. In that form only a pose message has to be sent for each position measurement.

[15]ROS package **robot_localization**. http://wiki.ros.org/robot_localization

Map Filter															
	x	**y**	**z**	**roll**	**pitch**	**yaw**	**vx**	**vy**	**vz**	**vroll**	**vpitch**	**vyaw**	**ax**	**ay**	**az**
IMU				X	X	X				X	X	X			
DVL							X	X	X						
VO							X	X	X	X	X	X			
Depth			X												
GPS	X	X													
USBL	X	X													

TABLE 3.2: Map filter inputs

Chapter 4

Tests

This chapter presents all the most representative factors concerning the different tests that have been performed. The objective of the tests is to extract reliable data with which evaluate and validate the developed positioning system. In order to do so, the experiments seek to find measures for the analysis of the precision and accuracy of the proposed localization system. Moreover, it is important to mention that since the USBL is assumed to be a factory calibrated system, no calibration procedure has been performed and all the measurements tests with the raw measurements, and the acoustic source level has been set to $-12dB$.

It is also important to recall the difference between precision and accuracy. Accuracy refers to the closeness of a measurement to the real value, whereas precision refers to the measurements closeness.

Measurement dispersion is analyzed in section 4.1 to determine the precision of the system when the vehicle and the USBL are supposed to be static. For that propose the USBL has been properly moored in order to minimize movements produced by the currents, and the AUV commanded keep its position autonomously while the static measurements were taken. This set up has several sources of error, the real displacements of both the AUV and USBL, so the obtained dispersion is considered as an upper bound of the precision. In any case, the error produced by the AUV displacement is estimated with an EKF in which we will integrate visual odometry from the stereo cameras, as well as the DVL and the rest of DR sensors.

Then, the proper performance of the USBL system and the integration on an EKF filter has been tested performing a survey mission of $225m$. The validation of the system is first tested in simulation, using the UWSIM, Prats, 2012, in order to use a simulated ground truth (GT) to evaluate system errors. It has been an useful tool to test USBL performance during development stages as well as tuning and validating measurement covariances for filter convergence before field tests. In fact, sensor measurements are simulated with Gaussian noise estimated from real sensor data.

Secondly, the positioning system is evaluated when performing the same survey mission during field tests. As stated before, in order to get the accuracy of a measurement, we need a real measurement value, a GT. Furthermore, we do not need only a punctual GT, but also a trajectory GT to be able of evaluate the integration of the measurement in the filter. Since we are dealing with an absolute positions it is no enough to have a really confident estimation of point in a trajectory path. Both, the sensor measurement and the output of the filter should be analyzed along a trajectory. Hence, we present a field test data set that will contain an approximation to a trajectory GT, a visual based SLAM with a feature rich bottom and many loop-closings.

FIGURE 4.1: Testing area.

All the field tests were performed at the north-west of Mallorca, in the Valldemossa harbor 4.1, shallow water with depth around $4m$. Communications with the AUV were performed using the catamaran buoy with the WLAN link in order to have a constant motorization of the stereo camera images, anyway, the position estimated by the USBL device was transmitted acoustically to the robot in order to test the positioning system when the estimation is delayed, updated with the odometry. Moreover, the robot sent navigation status information acoustically back to the ground station in order to seize part of the bandwidth, and limit the acoustic positioning measurements frequency.

4.1 Static precision

The analysis of the system precision is needed in order to know how confident we are about a measurement. It has been used to associate a covariance value to the measurement, and to compare with the precision obtained with the rest of the experiments.

For this experiment we have tried to fix both, AUV and USBL system, with the objective of obtaining the measurement dispersion in a setup where we can assume that a real distance is fixed. If the fixed distance where truly known we could talk about accuracy, but that's not the case. Then, from this experiments we will be able to get measurement dispersion, but not measurement offsets.

The set up for this experiment consists on the working set up presented in section 3.1. The USBL buoy has been properly moored with three cords in order to limit possible movements. In contrast, the AUV has been used with his own odometric navigation to conduct an straight path with $90s$ waits in way-points distributed evenly every $15m$, figure 4.2. Only the horizontal components of the position measurements have been considered, since the vertical component is very noisy and the depth measurement of the pressure sensor already provides a really good estimation.

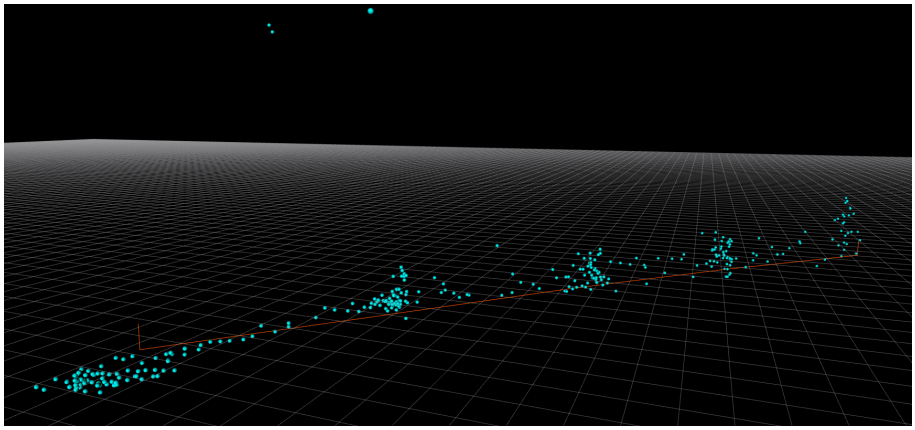

FIGURE 4.2: Trajectory data-set for precision estimation.

Since the robot is non-holonomic, the AUV has not control over all the DOF, it can not control the lateral displacements caused by external forces. This forces, as well as the controller errors on the DOF the the robot controls when the robot is commanded to maintain position, will cause some movement that has to be measured in order to be compensated. This has been estimated with a visual odometry (VO) aided EKF.

For each distance, the VO movement estimation has been obtained using the EKF implemented in the robot localization ROS package Moore, 2014, already integrated in the AUV architecture, using as an input the VO from an image tracker based on the ORB descriptor, DVL and the rest of DR sensors. This VO aided EKF is considered as a ground truth for two reasons; the displacements occurred during each keep position way-point are very small, and there is a feature rich seafloor with many static visual correspondences.

Figure 4.3 shows the estimated movement and the obtained USBL measurements, a distance error is obtained between each USBL measurement and the EKF estimated position at the USBL measurement time, this will be used as the AUV static error distribution. Outliers have been filtered using a distance threshold.

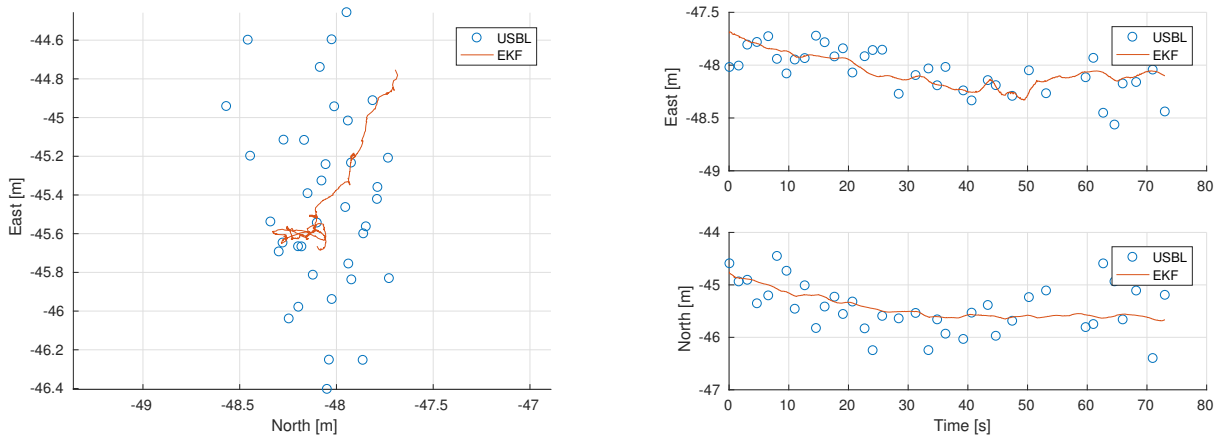

FIGURE 4.3: USBL measurements and EKF movement estimation. Test 3/5, at 66m distance

Static error distribution is presented in figure 4.4, as stated, they are the point-to-point error between USBL and EKF trajectories. From this error distributions the dispersion in the principal direction of each data set is shown, the maximum eigenvalue. From the figure it can be inferred that the measurement dispersion might be proportional to the relative distance between devices.

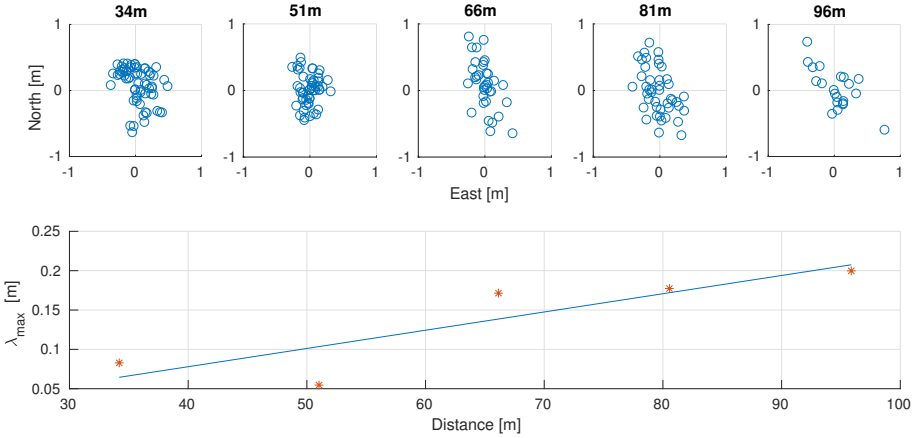

FIGURE 4.4: Data collection for the precision experiment. Up, movement compensated dispersion of the USBL measurements for the different data sets taken at five distances. Down, maximum eigenvalue of each data set with a linear regression $y = 0.0023x - 0.0148$

This results show that the estimated value of the dispersion will be at most $\sigma = 0.45m$ for distances smaller than $100m$, obtained from the upper bound given by the dispersion in the fifth measurement test $\lambda_{max} = 0.2$. The linear regression of the maximum eigenvalues presented in figure 4.4 provides an estimation of the slant range precision of $y = 0.0023x - 0.0148m$ in the studied distance range $[34 - 96]m$.

Although the analysis of a larger data set would definitively improve the statistical accuracy, it has been considered that for the scope of the project it is enough to approximate an upper bound for the precision error of the USBL system, in order to be combined with a safety factor to estimate the uncertainty associated to each measurement.

4.2 Survey

The orange grid of the figure 4.5 represents the survey mission that has been executed for this experiment, in simulation and in field tests. It is a grid of $15x15m$, with an area of $225m^2$, that consists in a $270m$ path. A survey is an usual exploration strategy for seabed image acquisition of a rectangular area with many loop-closings. The green dots are the USBL measurements and the blue trajectory is the output of a Kalman based filter that integrates odometric and absolute measurements.

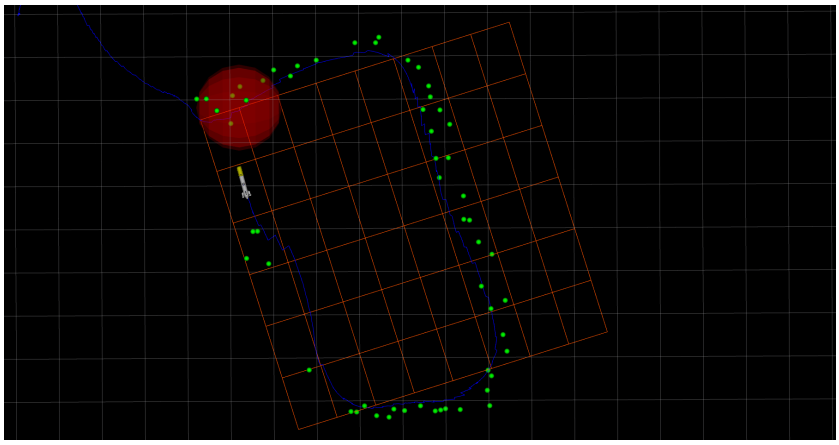

FIGURE 4.5: Survey mission performed in simulation and in field tests. A grid of $15x15m$, with an area of $225m^2$, that consists in a $270m$ path.

Sections 4.2.1 and 4.2.2 use the set of inputs detailed on the implementation section 3.4, for the so called odom filter, which contains continuous measurements, and the map filter, which also includes absolute measurements. Since visual odometry can not be gathered in all situations, for this evaluation it is not used as an input.

With respect to the kind of filter used, both data-sets have been tested using EKF and UKF estimation techniques. Even so, in order to ease the presentation of the obtained results, the validation and evaluation of the USBL system will proceed providing the results obtained only with the EKF approach, since it is considered the more generalized implementation. Afterwards, section 4.2.3 provides a comparison between the EKF and the UKF techniques when dealing with odometric and absolute position measurements.

4.2.1 Simulation test

During all the project development stages, simulation has been used as a previous step to field testing. The sensors have been simulated using the characteristics shown in table 4.1, they have added Gaussian noise estimated from real data with the given mean and standard deviation. Both GPS units are assumed to have white noise, being the world reference in the horizontal plane as well as the depth sensor in the case of the vertical reference. An offset has been added in the orientation of the IMU with respect to the reference. Both the yaw error produced by the compass, the angular speed error and the linear velocity error provided by the DVL will produce a drift in the dead-reckoning (DR) estimated trajectory. In the previous section has been obtained an upper bound estimation of the underwater positioning system error, $\sigma = 0.45m$. Then, it has been assumed that a fair uncertainty for the updated absolute measurement is has $\sigma = 0.40m$, which is the added uncertainty of the GPS buoy and the USBL relative uncertainty. The EKF implementation is tested with a default process noise covariance provided by *robot_localization* package authors.

The trajectories obtained for simulation are presented in figure 4.6; the simulated ground truth, the EKF output without absolute measurements, the EKF output that integrates the USBL measurements, and outlier free and updated USBL measurements.

Sensor	Period (Hz)	Delay (s)	Std	Mean
IMU(Orientation)	10	0	[0.001, 0.001, 0.001] rad	[0.005, 0.005, 0.06] rad
IMU(Angular speed)	10	0	[0.006, 0.006, 0.008] rad/s	[0.0, 0.0, 0.05] rad/s
Depth	10	0	[0.01] m	—
DVL	5	0	[0.03, 0.03, 0.03] m/s	[0.001,0.001, 0.001] m/s
GPS AUV	1	0	[0.1, 0.1, 0.1] m	—
GPS Buoy	1	0	[0.1, 0.1, 0.1] m	—
USBL	0.5	1	[0.3, 0.3, 0.3] m	—

TABLE 4.1: Simulated sensor performance.

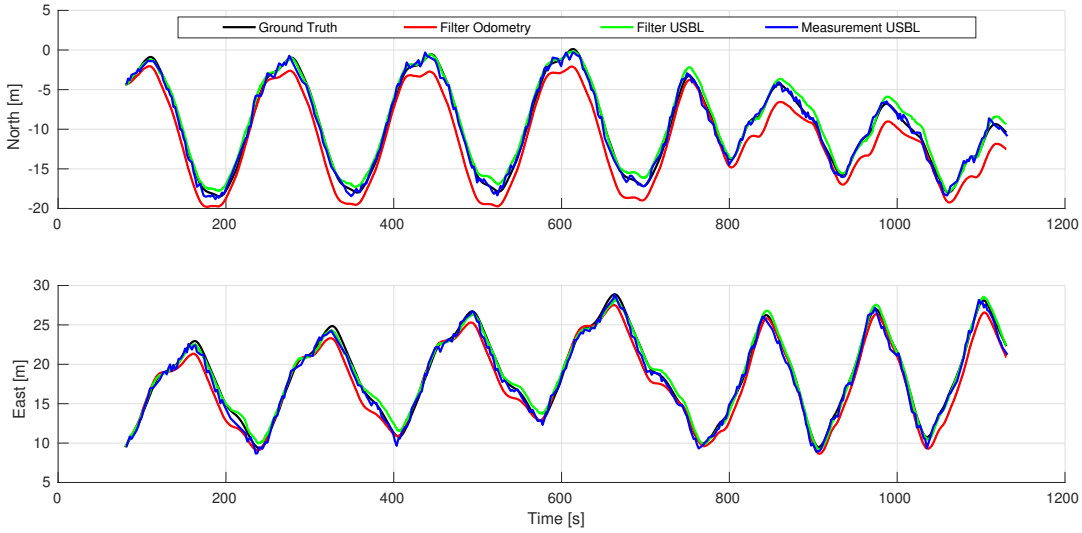

FIGURE 4.6: Trajectories from simulation.

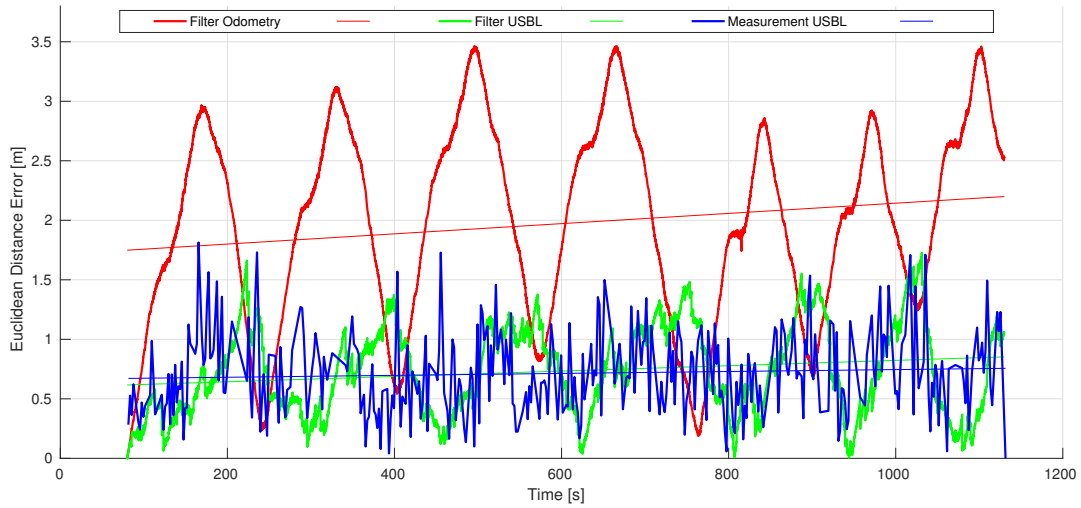

FIGURE 4.7: Euclidean distance error of the estimated trajectories and their linear regressions from simulation.

Figure 4.7, provides a better insight on the produced error between each trajectory with respect

to the GT. The odometric estimation lead to a large error peaks in the pose estimation caused by an accumulation of small errors in the movement estimation.

In any case, it is curious that the odometry pose estimation seems to have a bounded error when in real life it is well known that the odometry continuously accumulate errors that lead to an unbounded error growth. The position error should not grow when performing an straight line, but also when performing circular trajectories as it is the case of the survey mission commanded. The odometric trajectory error seems to grow bounded due to the introduction of a noise that only produce systematic error. In other words, the vehicle has a bias in the orientation, the angular and lateral speeds, then, when traveling in one direction the drift increases, but when it goes back the drift recovers since the error is produced in the opposite direction. The high frequency of the sensor updates combined with the slow dynamics makes the added Gaussian noise to be centered and cause a constant bias. Whereas in this case the odometry estimation error seems to be bounded (the growth rate is very small), the odometry error seems to be proportional to the survey size, in this case a $225m$ survey produces a maximum error of $3.5m$

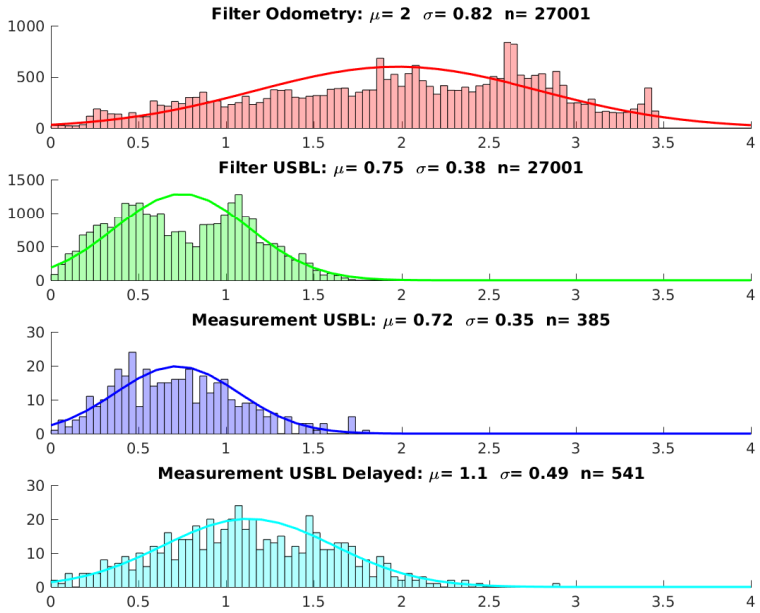

FIGURE 4.8: Final trajectory error distribution histograms from simulation.

The histogram of the trajectory error distribution of the studied trajectories is presented in figure 4.8. Please note that both, the mean and the standard deviation of the absolute position filter error is slightly bigger than the updated USBL measurement, in this case the a accumulated error show that the measurement error is more accurate than the multisensor fusion, but also note that the output of the filter provides a more continuous position estimation that is best suited for the navigation and control of the robot. The figure also presents the histogram of the USBL delayed measurements, realize of how the update and rejection stages improve the error dispersion at expenses of reducing a 29.3% the total number of 526 raw measurements.

This synthetic experiment shows that the trajectory error bound depends on the size of the survey mission, but not in the traveled distance when only systematic errors are present.

4.2.2 Field test

This experiment follows almost the same procedure than the previous but with one fundamental difference, the data-set used to analyze the performance of the positioning system comes from field tests. As previously commented, it has been a main concern along the project development to find a real GT when performing tests at sea. Many alternatives were proposed, but the lack of equipment and the need of testing in real environments made them unfeasible, recall that many acoustic artifacts may appear in real environments 2.3. The installation of a long baseline system, or the execution of the field tests in enclosed installations where a source of GT exist were not an option.

Hence, the vision based SLAM technique proposed by Negre, 2016 is proposed to be used as an approximate GT if some requirements are satisfied. The requirements relay on the feature richness of the sea bottom that determine the homography transformation precision between consecutive frames, as well as in the quantity and distribution of loop-closings used to optimize the pose graph obtained. In this experiment, having a mean of 112 inliers per image pair and 176 loop closings, the optimized path provided by the SLAM algorithm has been used as a GT, being aware that some drift may exist at the furthest parts of the survey relative to the origin.

In order to compare the trajectories, the visual based SLAM GT trajectory has been transformed to the EKF filter reference frame. Figure 4.9 shows the obtained trajectories: an EKF that integrates only odometric measurements, an EKF that also integrates an absolute positioning measure produced by the USBL system, and the provided by the updated USBL measurements. The odometric pose estimation progressively drifts leading to the large euclidean distance errors that are shown in the figure 4.10.

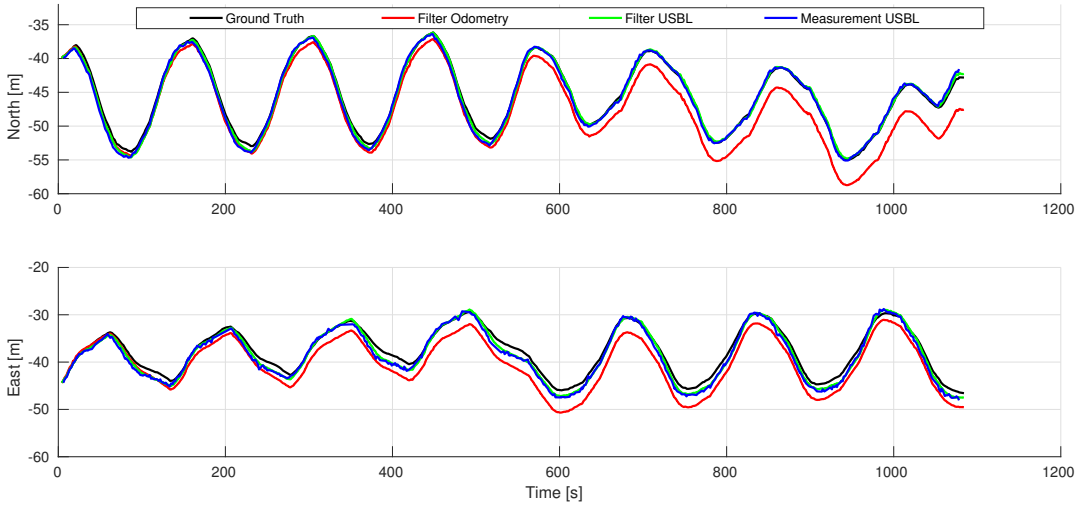

FIGURE 4.9: Trajectories from field test.

In contrast with the simulated experiment, in this case the odometry error clearly has an unbounded behavior caused by non-systematic errors, 1.8% of the total path length ($270m$). This kind of error may no be corrected nor calibrated since it is caused by chaotic phenomena that mostly appear in unstructured environments. In the case of the AUV it might be caused by sea currents or unstructured seafloor, which lead to noisy IMU and DVL measurements. As it was expected, the absolute measurement filter has a bounded error behavior. However, it has several error peaks that may be produced by an initial drift that bias the SLAM estimation.

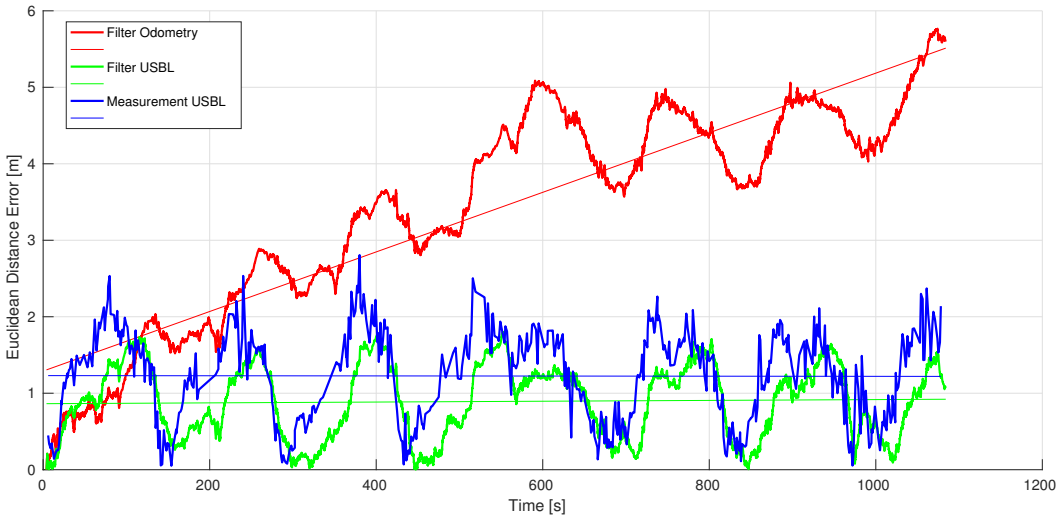

FIGURE 4.10: Euclidean distance error of the estimated trajectories and their linear regressions, from field tests.

In order to fully understand the odometry estimation error evolution, it is important to point out that during the first half of the survey mission the vehicle always perform clockwise turns. While in the second half the turns are performed counter-clockwise. It seems that the robot odometry produces an unbounded error drift in the first half and continues bounded in the second.

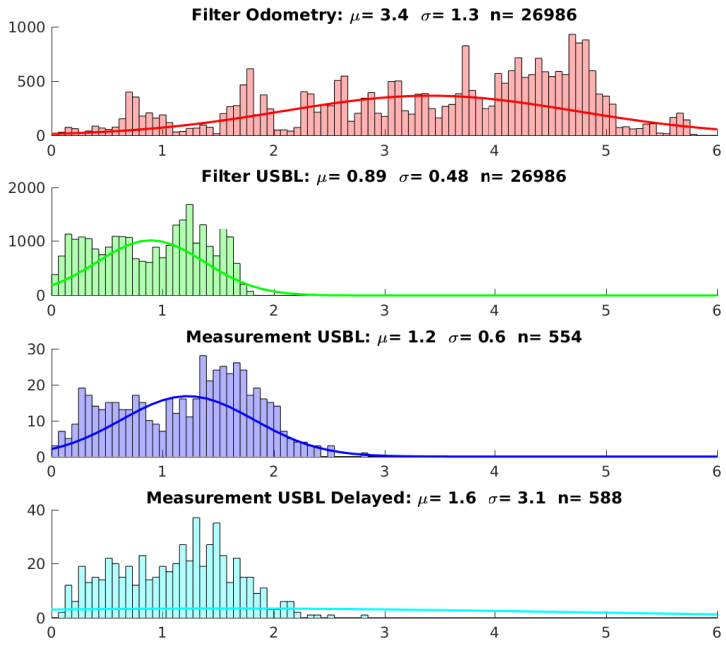

FIGURE 4.11: Final trajectory error distribution histograms, from field test.

The trajectory error distributions are presented in figure 4.11. First, it can be seen the correct performance of the outlier rejection and update of the raw USBL measurements. In fact, the rejection of almost the 6% measurements results in a significant improvement of the measurement accuracy and precision.

It has been reached a mean frequency of $0.5Hz$ USBL measurements, which provides sufficient transmission rate to send navigation status information back to the ground station. Besides, the distribution of the odometric estimation does not show any relevant information, since the error is constantly growing. However, in this case the output of the filter that includes absolute measurements shows a more robust behavior. In contrast with the simulation test, it is more accurate and precise than the updated USBL measurements.

Nonetheless, this representation only provides the error distribution at the end of the trajectory and it does not provide any idea of its evolution. Figure 4.12 represents the accumulated error evolution during all the trajectory time. The mean accumulated error is represented with a confidence interval of one standard deviation. It is shown that the fusion of motion with absolute measurements provide the most accurate results along all the trajectory. It shows the strength of multisensor fusion techniques.

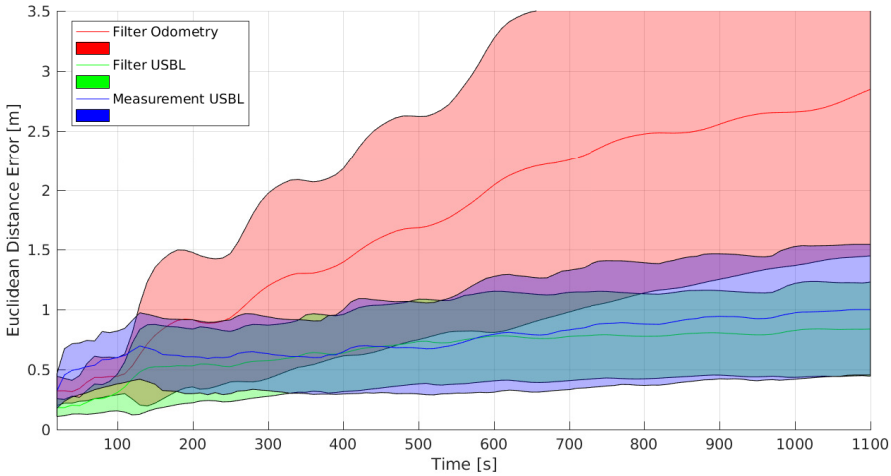

FIGURE 4.12: Accumulated trajectory error distribution histogram, from field tests.

4.2.3 Filters comparison

This section provides a comparison between EKF and UKF filtering techniques in the presence of multisensorial data provided for odometric and absolute measurements. As stated in the section 2.5, both filters assume a Gaussian error distribution. In the case of the USBL measurements, it has been shown in the previous tests that at long term they meet the Gaussian assumption, once the outliers have been rejected.

Regarding to the state propagation, EKF uses the mean and the variance as an state description that propagate onto a new state using the model jacobians. In contrast, UKF describes the actual state using several reference points used as statistical descriptors. Once the descriptors have been propagated using the model dynamics, a new Gaussian distribution can be fitted, and determine the new state and its associated uncertainty. Whereas EKF relays in a first order linealization of the model transition function, UKF avoids a direct linealization and captures the model state distribution up to a third order Taylor expansion. Therefore, rather than the EKF, UKF is supposed to estimate more accurately the new state distributions when the model transitions are highly non-linear.

As presented in figure 4.13 and 4.14, the difference obtained with the gathered field test data results very small. Whereas UKF seems to have an more accurate trajectory error distributions, it shows a growing error trend that might deteriorate the behavior. In any case, the proposed ground truth for validation and evaluation of the USBL system can not be considered accurate enough to evaluate which filter provides a better performance.

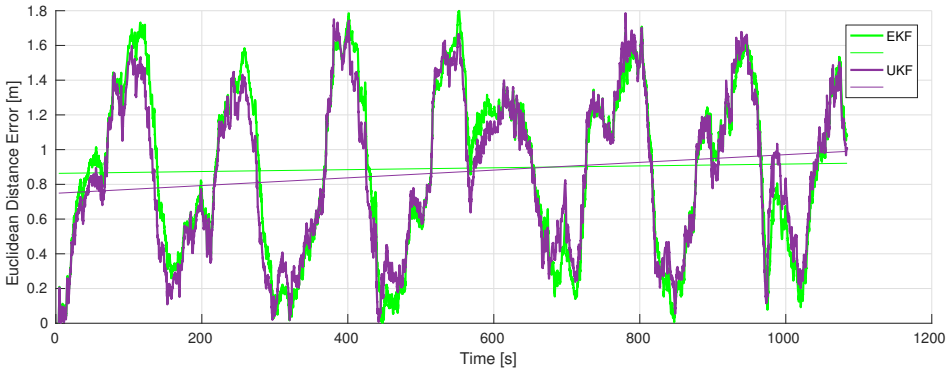

FIGURE 4.13: Euclidean distance error of the EKF and UKF estimated trajectories, from field tests.

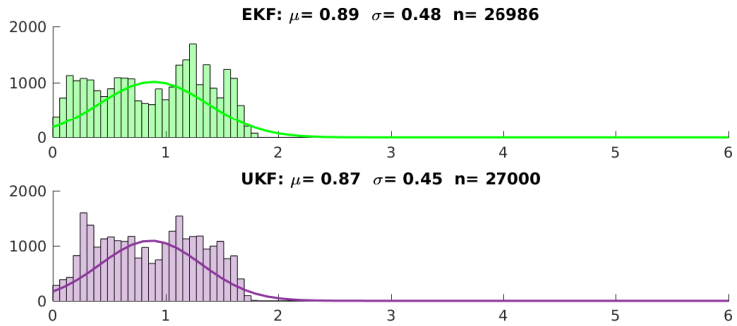

FIGURE 4.14: Final trajectory error distribution histogram, from field tests.

Nevertheless, it is important to see that the minimal difference relaying on the kind of Kalman filter used may relay in that non-linearities are very soft, and the implementation of other filtering techniques, such as particle filters, might not be justified.

Chapter 5

Budget and Impact

5.1 Budget

This section details the costs associated to the development of this project. The costs are classified in four types: hardware, software, human resources and general expenses.

Hardware resources In this part we fit all the costs related with the operation of the robot and field test underlying equipment, detailed in table 5.1. Using the quantity, the unit price, the amortization period and the hours of use the cost associated to each specific resource may be obtained. Considering a 40 hours per week and 52 weeks per year, the total cost estimated for hardware resources is 1,415.90 €.

Resource	#	Unit Price	Amortization period	Price per hour	Hours of use	Amortization
Sparus II	1	50,000.00 €	5	19.23 €	163	783.65 €
USBL	1	25,000.00 €	5	2.40 €	163	391.83 €
PC	5	1,500.00 €	3	0.24 €	849	204.09 €
Wifi Link	1	150.00 €	5	0.01 €	123	1.77 €
Router	1	30.00 €	3	0.00 €	123	0.59 €
Testing Pool	1	200.00 €	3	0.03 €	40	1.28 €
Car	2	3,500.00 €	5	0.34 €	48	16.15 €
Trailer	1	500.00 €	5	0.05 €	24	1.15 €
Shade Canopy	1	100.00 €	3	0.02 €	123	1.97 €
Table	1	80.00 €	3	0.01 €	123	1.58 €
Chairs	5	30.00 €	3	0.02 €	615	11.83 €
TOTAL						**1,415.90 €**

TABLE 5.1: Hardware resources

Figure 5.1 shows the most representative hardware costs, the robot represents the most important cost, being a 55% of the total. The USBL device also suppose an important part of the cost, a 28% approx.

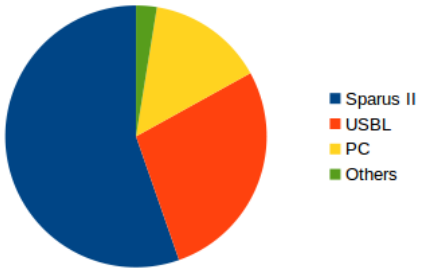

FIGURE 5.1: Hardware resources cost proportions

Software resources All software used for this project has been Open Source, therefore no associated costs can be attributed to this part. Table 5.2 shows a list of the software used.

Resource	Unit Price
Ubuntu 14.04LTS	0.00 €
ROS Indigo	0.00 €
Sublime editor	0.00 €
UWSim	0.00 €
COLA2	0.00 €
Evologics	0.00 €
Other libraries	0.00 €
TOTAL	**0.00 €**

TABLE 5.2: Software resources

Human resources Although this project has been associated to a lab technician, other four researchers have been involved in it. The interest on the project as well of the basis of it and the supervision was provided by the director of the research group, working as a project manager[1]. Besides, a coordinator was needed to provide some technical guidance and to help developing the main ideas, as well as to arrange field tests, with an associated research scientist[2] associated salary. Other support has been provided by a lab technician[3] with great expertise about implementation of underwater robotic systems. Also, a lab assistant[4] has been in charge of the construction of the different prototypes, and has assisted on the sea trials. Hourly wages, total hours of work and the total cost associated to all human resources is detailed in table 5.3, it results in a total cost of 15,143.24 €.

Position	Gross annual salary	Hourly wage	Hours of work	Cost
Project Manager	79,210.00 €	39.29 €	10	392.91 €
Research Scientist	72,980.00 €	36.20 €	93	3,366.64 €
Lab Technician 1	33,820.00 €	16.78 €	143	2,398.94 €
Lab Technician 2	33,820.00 €	16.78 €	420	7,045.83 €
Lab Assistant	21,360.00 €	10.60 €	183	1,938.93 €
TOTAL			**849**	**15,143.24 €**

TABLE 5.3: Human resources

The chart in figure 5.2 represents the cost proportions expended in human resources.

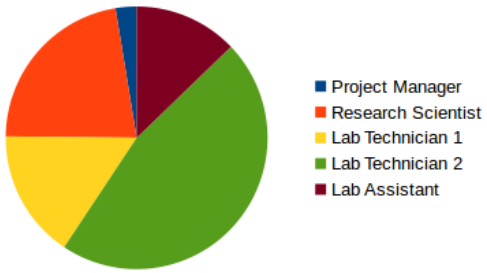

FIGURE 5.2: Human resources cost proportions

[1]Project manager gross annual salary average. http://www.indeed.com/salary/Project-Manager.html
[2]Research scientist gross annual salary average. http://www.indeed.com/salary/Research-Scientist.html
[3]Lab technician gross annual salary average. http://www.indeed.com/salary/Lab-Technician.html
[4]Lab assistant gross annual salary average. http://www.indeed.com/salary/Lab-Assistant.html

General expenses In general expenses are included the rest of costs, the most relevant ones are the power consumption, oil[5] for the cars and the electric generator and lab electricity[6], and the costs associated to a project field experiments travel to Girona and a conference in Germany, flights, diets, beds and car renting. It represents 1,978.50 € cost.

Concept	Quantity		Unit Price	Cost
Gasoline	20	l	1.20 €	24.00 €
Electric energy	630	kWh	0.15 €	94.50 €
Diets	14	ud	30.00 €	420.00 €
National plane tickets	4	ud	100.00 €	400.00 €
International plane tickets	2	ud	170.00 €	340.00 €
Hotel	14	ud	50.00 €	700.00 €
TOTAL				**1,978.50 €**

TABLE 5.4: General expenses

Total cost Then, the total costs that might be associated to the project are shown in table 5.5, and represented in figure 5.3. As stated before software resources does not suppose any cost since only open source software has been used. It is important to realize that even with high tech equipment expenses human resources represent the biggest cost they represent the knowledge and expertise of the project. Notice the big proportion that represents the human resources part, almost the 82% of the total.

Resource	Cost
Hardware	1,415.90 €
Software	0.00 €
Human	15,143.24 €
General	1,978.50 €
TOTAL	**18,537.64 €**

TABLE 5.5: Total costs associated to the project

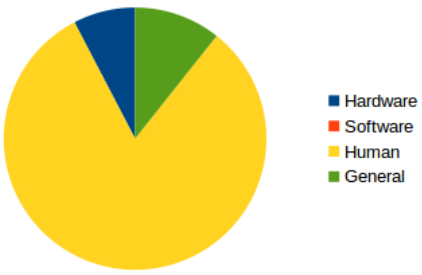

FIGURE 5.3: Total costs proportions

[5]Spanish oil cost estimation. http://servicios.elpais.com/gasolineras/
[6]Spanish electricity cost estimation. http://www.tarifadeluz.com/hoytg.php

5.2 Impact

The social economic impact of this work can not be evaluated directly, but together with the final applications in which it is based. This project improves the localization of the Turbot AUV, which affects directly to the navigation and in the scene reconstruction of the projects presented in section 1.3, it improves the robustness to the robot missions as an step to simplify its use for final applications. This evaluation will have also a local perpective, containing justifications from the *Plan for Science, Technology, Innovation and Entrepreneurship Balearic Islands 2013-2017* PCTIE document, Illes Balears, 2012, and the *Innovation Strategy for Smart Specialisation RIS3. Specialization diagnosis of Economic, Technological and Scientific Balearic Islands* RIS3 document, Bit, 2014, which detail the milestones looking for an economy able to generate a high added value and growing welfare for the Balearic Islands society.

5.2.1 Social

Visual maps, in 2D or are tools with added value that are being extensively used in museums, Google street-view[7], videogames, scene reconstruction, etc. Nowadays is difficult to have this kind of representation of underwater environments, which could be used this environments for both, researchers and general public, to educate and promote good practices on environmental issues. Besides, the recovery and conservation of archaeological wrecks suppose a great potential impact for the preservation of the underwater cultural heritage, commonly, the best conserved wrecks are the ones that are not accessible to scuba divers, since they have a escaped from pillage. This project has a great implication in the following strategic areas defined in the PCTIE.

Marine Science and Technology The Balearic Islands autonomic community has more than 1700km of coastline, with which it has a strong dependence. This natural resource is accountable for the 70% of the GDP. Therefore, the PCTIE emphasize the necessity of preserve, recover and manage with the advanced knowledge provided by the latest scientific advances. In that direction, the construction of more extensive, precise and complete 2D maps will be a tool to have a better motorization of the sea bed, for example to control the Posidonia Oceanica extension. The acquisition of bathymetries on shallow waters would be cheaper and quicker than using traditional acoustic methods. All this improvements would not be possible without a proper robot localization system as an step for an easy and efficient monitor tool to manage the Balearic coastline. This work procure three objectives proposed by the document.

- Contributes on the consolidation of the research activities of the Balearic Islands.
- Promotes technology development and knowledge transfer.
- Fosters scientific and technical training and dissemination.

Tourism The PCTIE regards about the importance of the cultural heritage as a resource that contributes to create a good vision of the Balearic community, making a difference with other competing destinations. 2D or 3D seabed reconstructions could be very attractive tools for the general public, the virtual visit of specially rich underwater environments could be of a great value for the different touristic promotion platforms in order to improve the reputation of the place. Moreover, visual reconstructions in regions of special archaeological or cultural interest could be used as a distinctive asset to promote diving and cultural tourism, with an added value and less environmental impact than the traditional tourism.

It is important to mention that the system under development that has been the focus of work of this project will increase the vigilance and study of the marine environment, which will directly impact on the touristic product offered.

[7] Google street-view. https://www.google.com/streetview/

5.2.2 Environmental

It is essential a proper preservation of the Balearic Islands natural wealth for both, the population and the tourism industry competitiveness since it is its main resource. The PCTIE steps forward for the biological diversity conservation, specially for the endemisms.

As stated in section 1.3, one of the main uses of the AUV is for research on projects related with surveillance of the Balearic Islands shallow waters, to map the sea bottoms and gather data about Posidonia Oceanica (PO) meadows characteristics, a seagrass endemic to the Mediterranean Sea. Bottom coverage is the main used descriptor for biologists and it is which is currently being used for data gathering. The ongoing projects have the propose of building an effective and cost efficient tool to monitor PO meadows in different spaced moments in order to evaluate changes in extension and jointly with other indicators, such as temperature an salinity, be able to explain the causes of it.

PO meadows are identified as a priority habitat type for conservation by the European Community (Dir. 92/42 CEE 21/05/92 and 97/62/CE 27/10/1997), Díaz-Almela, 2008. According to Jordà, 2012, PO meadows are very important for carbon burial, nutrient cycling, coastal protection from erosion and enhanced biodiversity. It is one of the plant species on the biosphere with the longest lifespan, having shoots that live up to the 50 years, and the slowest growing rate, $1 - 6cm$ per year. They assess the seagrass evolution with respect to different perspectives about climate warming and local pressures caused by human, concluding that in the year 2049 PO will reach the 10% of the present density if the actual mortality rates caused by global warming and anthropogenic pressures continue.

Balearic Islands local newsletters are increasing the attention to this issue that might become an economical and social problem in a short period of time because of the local dependence in the sea water quality. Some examples are the published information related with the decreasing of PO extension due to anthropogenic pressures [8], and due to an organic matter excess caused by non-properly purified waste water spillage[9].

5.2.3 Economic

This section will review some important economical figures related to the underwater robotics, specially to AUVs. Global Unmanned Underwater Vehicles (including ROVs and AUVs) market is growing at a CAGR of 20% in terms of unit shipment over the period 2014-2019 Reuters, 2014. The ROV market was estimated at 1.2 Billion$ in 2014 registering a 20% CAGR in 2019. The global AUV market was estimated to be $457 million in 2014 and is expected to register an even higher CAGR of 32% in 2019.

The report identifies SAAB (Sweden), Fugro (The Netherlands), Oceaneering (U.S.) as the market leaders that occupy a significant market share for ROV. Kongsberg (Norway), Teledyne (U.S.), Bluefin Robotics (U.S.), and Atlas Elektronik (Germany), are identified as the leaders in the AUV market.

The most-likely scenario forecast for 2018, reported in the World AUV Market Report Dormer, 2014, estimates an AUV fleet of 903 units (285 large, 348 Medium and 270 for small vehicles).

A direct impact is related to the final applications based on marine archaeology, based on a time saving base, since operations will be done faster, more work will be done with the same resources. The cultural heritage agency from Catalonia estimates that a common operation at sea involves 4 archaeologists, 2 sailors and 1 captain. Operations campaigns take place during about 120 days at sea, from boats of at least 20m length, with a lower bound of a daily cost of 5000€. With the introduction of automated vehicles to perform deeper more work could be done and the operational cost could be reduced as well as augment the productivity.

Future trends in marine robotics Zhang, 2015, point in the direction of adding external localization systems, acoustic based to obtain accurate localization in long term missions, it becomes a necessary feature for underwater robotic system competitiveness.

[8] Spanish local newsletter about anthropogenic pressures over Posidonia Oceanica. *El organismo vivo más grande del mundo se muere*. http://www.elmundo.es/baleares/2016/09/04/57caf4bd46163f842c8b4602.html

[9] Spanish local newsletter about an organic matter excess in the Balearic Islands. *La plaga de bacterias que extermina el fondo marino en la cloaca de Palma*. http://www.elmundo.es/baleares/2016/09/16/57dc0d03ca4741b3398b458a.html

Chapter 6

Conclusions

Many experience have been obtained from the execution of this project. Whereas the implantation of an acoustic device for positioning and communication may not have an extensive theoretic complexity, grate part of it's difficulty relays in the practical implementation. The simulation has been used to test the system in ideal conditions, as a first step to have an easy validation. Real world trials, particularly in marine environments, have been shown to be extremely harsh for sensor data gathering and for proper performance of the vehicle. Not to mention that the uneven conditions of marine environments severely difficult the execution of engineering tasks.

The difference on the planning proposed at the beginning of the project, and the real execution shown in the appendix A, reflects some of the constraints a marine environment may arise. Not only bad weather conditions, but also problems in the build-in hardware that a tiny torpedo shaped AUV have. Which is compactly enclosed, subject to many waterproofed connections, and left in a harsh and hazardous environment. Underwater autonomous robotics are in a young stage of development, it will require of the implementation of more robust and general techniques for maturing and overcome the board range of situations in which an AUV must perform. The installation of the USBL system is considered as a fundamental step in that direction.

For the total integration of the USBL system it has been expended approximately the same time that was planned. On the contrary, it's validation using a ground truth (GT) has taken longer than expected. Since the beginning, it has been a requirement to test the system in a real environment for two reasons: the nature of long range acoustics, and the limited scientific documentation on such a field test evaluation. Once discarded many GT alternatives, due to the lack of important infrastructure and technological resources, it was decided to do the validation using the other source of absolute position measurements that the robot has when is close to the seafloor, a visual based SLAM, since it has been shown to have a minimal error.

Once it has been decided how to capture a GT, the USBL system has been tested in one of the worst situations, acoustically speaking, in which the robot will perform: shallow waters $4-6m$ depth in a small bay, with a quite unstructured seafloor formed by rocks. On the contrary, the conditions were very good for the visual based SLAM GT: a feature rich seafloor, with an appropriate sun light condition.

Assuming that the captured data-sets are long enough, and that the USBL and SLAM trajectory errors do not cancel each other systematically, this kind of GT allows to determine an upper limit for the USBL positioning system error of $0.9m$. This result means that the fusion of USBL system measurements sets a bound to the error, even using the odometry to update the USBL delayed measurements. Therefore, the integration of such an absolute measure improves the navigation, allowing larger survey missions without drift. Moreover, the pose estimation provides improved reference for the sensor data. For instance, it is further used to build seabed reconstructions, even when the images or the trajectory do not satisfy the visual based SLAM minimum requirements, figure 6.1.

In conclusion, this Thesis has improved the autonomy of the Turbot AUV to perform larger and deeper missions, with an increased degree of safety and robustness. Besides, it has provided to the underwater robotic community, three software packages for the acoustic and positioning system implementation of an USBL: an acoustic link for communication, a modified driver as a bridge between the Evologics device and ROS, and a pipeline to treat delayed measurements a and insert them in a filter.

Moreover, an experimental assessment has been performed to evaluate the USBL system behavior in field test, providing an upper bound for the accuracy and precision using a visual GT. It is considered, that the time and resources expended in the project development are rather small compared to the great social, environmental and economical repercussion that the development of new techniques to explore the oceans will have.

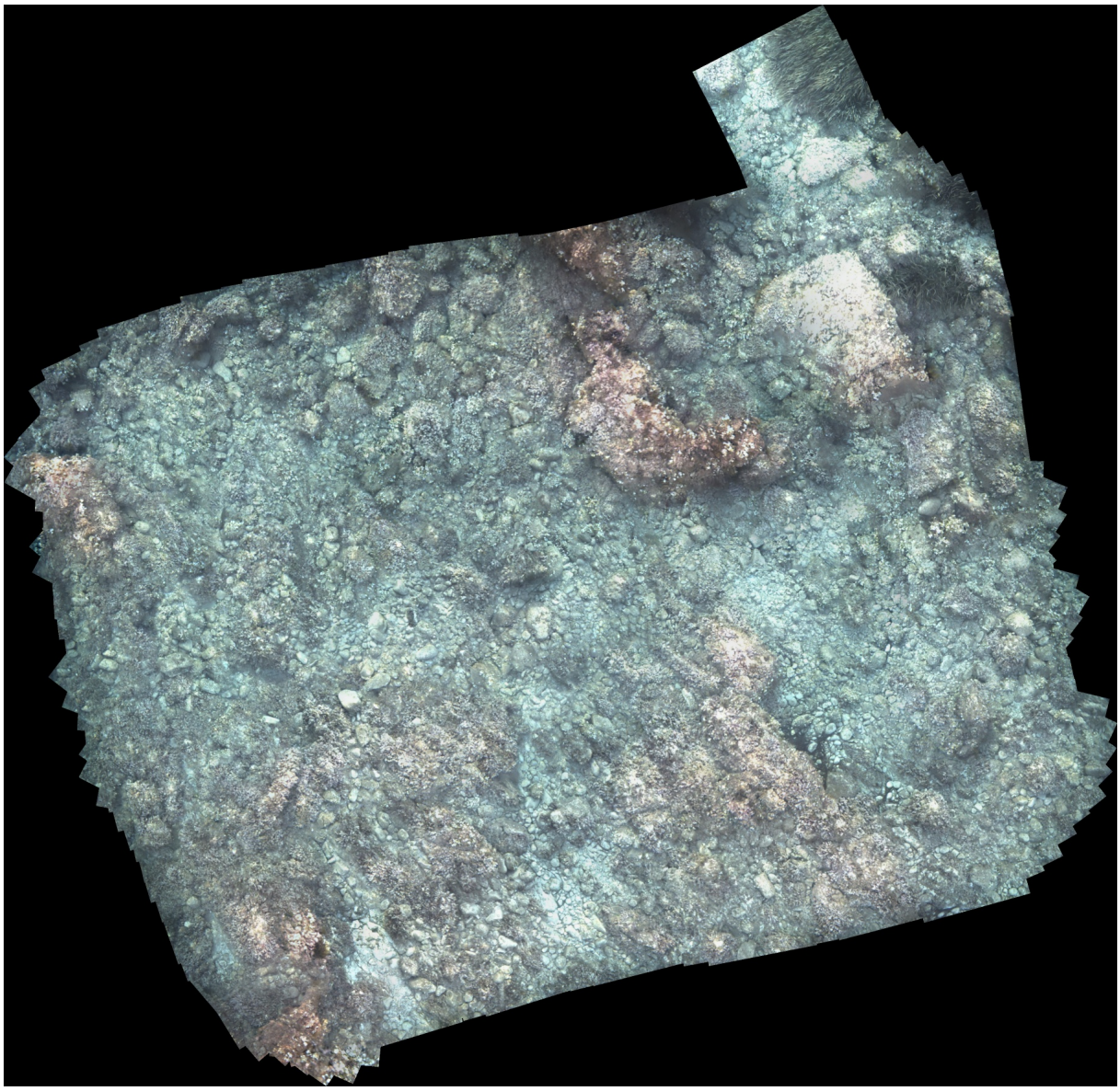

FIGURE 6.1: 2D reconstruction obtained from the field test data-set. Obtained using the pose estimation of the absolute positioning filter without using visual SLAM.

Appendix A

Schedule

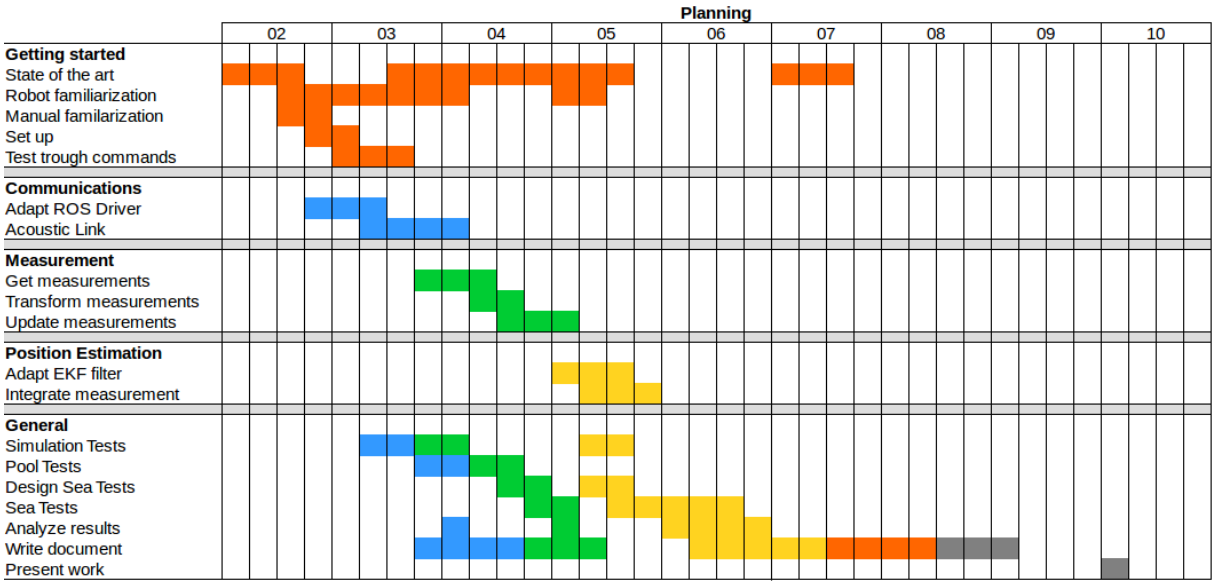

FIGURE A.1: Initial planning of the project

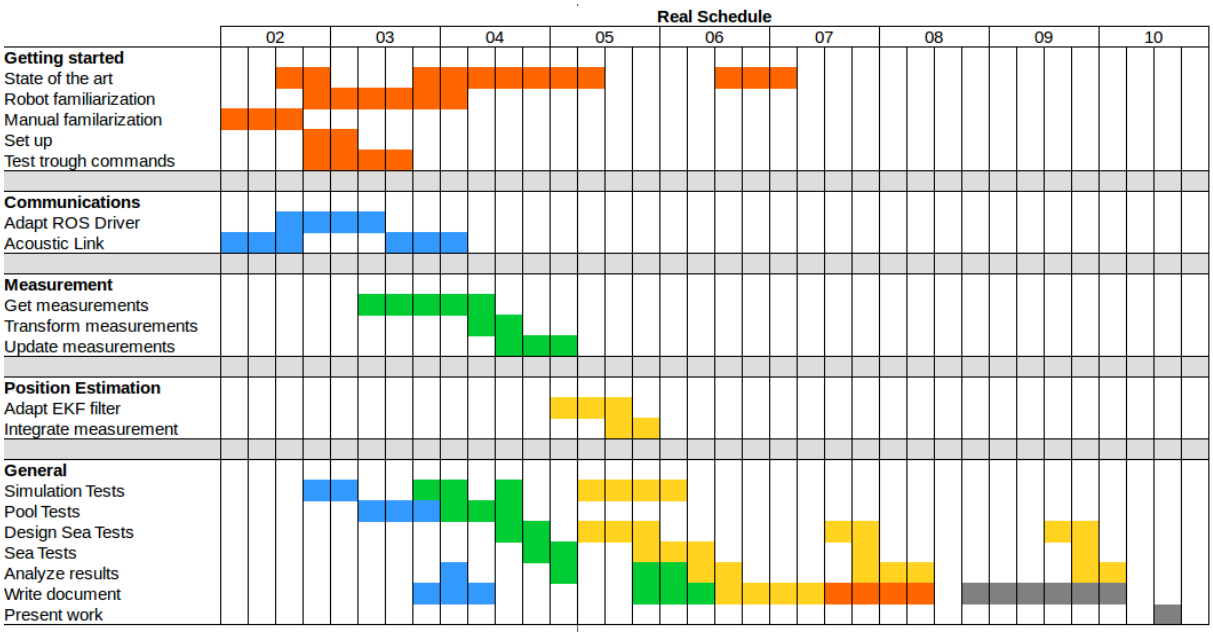

FIGURE A.2: Real schedule of the project

Appendix B

Sensor Specifications

B.1 USBL - EvoLogics S2CR 1834

EvoLogics®

USBL POSITIONING AND COMMUNICATION SYSTEM

S2CR 18/34 USBL

PRODUCT INFORMATION

Simultaneous positioning and communication

S2C Technology: accurate 3D positioning and reliable data transmissions with up to 13.9 kbit/s

Horizontally omnidirectional beam pattern, optimized for medium range operations in reverberant shallow waters

TECHNICAL SPECIFICATIONS

GENERAL	OPERATING DEPTH	Delrin	200 m
		Aluminium Alloy	1000 m
		Stainless Steel	2000 m
		Titanium	2000 m
	OPERATING RANGE		3500 m
	FREQUENCY BAND		18 - 34 kHz
	TRANSDUCER BEAM PATTERN		horizontally omnidirectional
USBL	SLANT RANGE ACCURACY [1]		0.01 m
	BEARING RESOLUTION		0.1 degrees
	NOMINAL SNR		10 dB
CONNECTION	ACOUSTIC CONNECTION		up to 13.9 kbit/s
	BIT ERROR RATE		less than 10^{-10}
	INTERNAL DATA BUFFER		1 MB, configurable
	HOST INTERFACE [2]		Ethernet, RS-232 (RS-485/422*)
	INTERFACE CONNECTOR		up to 2 SubConn® Metal Shell 1500 Series
POWER	CONSUMPTION	Stand-by Mode	2.5 mW
		Listen Mode [3]	5 - 285 mW
		Receive Mode [4]	less than 1.6 W
		Transmit Mode	2.8 W, 1000 m range
			8 W, 2000 m range
			35 W, 3500 m range
			80 W, max. available
	POWER SUPPLY [5]		External 24 VDC (12 VDC*) or internal rechargeable battery*
PHYSICAL	DIMENSIONS [6]	Housing/USBL sensor	Ø 110 mm x 170 mm / Ø 130 mm x 145 mm
		Total length	315 mm
	WEIGHT dry/wet	Delrin	5775/730 g
		Aluminium Alloy	5500/1800 g
		Stainless Steel	13130/6130 g
		Titanium	9830/4830 g

* optional
[1] Slant range estimation is based on the measured time delay, slant range accuracy depends on sound velocity profile, refraction and signal-to-noise ratio.
[2] See the Configuration Options for available standard interface combinations.
[3] User-configurable Listen Mode is only available with a Wake-Up module installed. Power consumption in Listen Mode depends on Listen Mode settings.
[4] Power consumption for the RS-232 interface option. Add 600 mW for the Ethernet interface option.
[5] Contact EvoLogics for more information on power supply options.
[6] Dimensions of a Delrin housing, other builds are slightly larger.

tel.: +49 30 4679 862 - 0
fax: +49 30 4679 862 - 01
evologics.de
sales@evologics.de

B.2 Modem - EvoLogics S2CR 1834

UNDERWATER ACOUSTIC COMMUNICATION SYSTEM

S2CR 18/34

PRODUCT INFORMATION

S2C Technology: fast and reliable data transmissions with up to 13.9 kbit/s

Advanced data delivery protocol

Horizontally omnidirectional beam pattern, optimized for medium range transmissions in reverberant shallow waters

TECHNICAL SPECIFICATIONS

GENERAL	OPERATING DEPTH	Delrin	200 m
		Aluminium Alloy	1000 m
		Stainless Steel	2000 m
		Titanium	2000 m
	OPERATING RANGE		3500 m
	FREQUENCY BAND		18 - 34 kHz
	TRANSDUCER BEAM PATTERN		horizontally omnidirectional
CONNECTION	ACOUSTIC CONNECTION		up to 13.9 kbit/s
	BIT ERROR RATE		less than 10^{-10}
	INTERNAL DATA BUFFER		1 MB, configurable
	HOST INTERFACE [1]		Ethernet, RS-232 (RS-485/422*)
	INTERFACE CONNECTOR		up to 2 SubConn® Metal Shell 1500 Series
POWER	CONSUMPTION	Stand-by Mode	2.5 mW
		Listen Mode [2]	5 - 285 mW
		Receive Mode [3]	less than 1.3 W
		Transmit Mode	2.8 W, 1000 m range
			8 W, 2000 m range
			35 W, 3500 m range
			80 W, max. available
	POWER SUPPLY [4]		External 24 VDC (12 VDC*) or internal rechargeable battery*
PHYSICAL	DIMENSIONS [5]	Housing	Ø 110 mm x 170 mm
		Total length	265 mm
	WEIGHT dry/wet	Delrin	2445 / 400 g
		Aluminium Alloy	2170 / 1470 g
		Stainless Steel	9800 / 5800 g
		Titanium	6500 / 4500 g

* optional
[1] See the Configuration Options for available standard interface combinations.
[2] User-configurable Listen Mode is only available with a Wake-Up module installed. Power consumption in Listen Mode depends on Listen Mode settings.
[3] Power consumption for the RS-232 interface option. Add 600 mW for the Ethernet interface option.
[4] Contact EvoLogics for more information on power supply options.
[5] Dimensions of a Delrin housing, other builds are slightly larger.

tel.: +49 30 4679 862 - 0
fax: +49 30 4679 862 - 01
evologics.de
sales@evologics.de

B.3 DVL - Teledyne ExplorerDVL Piston

Operational Specifications

	Phased Array	Piston Array
Bottom Tracking		
Maximum Altitude [1] [3]	81m	66m
Minimum Altitude	0.5m (0.31m optionally)	0.5m (0.25m optionally)
Velocity Range [2]	±9.5m/s	±17.0 m/s
High Accuracy Bottom Track Long Term Accuracy [6]	±0.3% ± 0.2cm/s	±0.5% ± 0.2cm/s
Basic Bottom Track Long Term Accuracy [7]	±1.15% ± 0.2cm/s	
Precision @ 1 m/s [4]	±1.0cm/s	±1.0cm/s
Precision @ 3 m/s [4]	±1.8 m/s	±1.9cm/s
Precision @ 5 m/s [4]	±2.6 cm/s	±2.8 cm/s
Resolution	0.1cm/s (default), 0.001cm/s (selectable)	0.1cm/s (default), 0.001cm/s (selectable)
Ping Rate	12Hz max	12Hz max
Water Profiling		
Maximum Range [1] [3]	35m	25m
Minimum Range	1.33m	1.33m
Velocity Range [2]	±12 m/s	±12 m/s
Long Term Accuracy	±0.3% ± 0.2 cm/s	±0.5% ± 0.2 cm/s
Precision @ 1m/s and 2m bin size [4]	±4.7cm/s	±2.3cm/s
Precision @ 3m/s and 2m bin size [4]	±4.8 cm/s	±2.5 cm/s
Precision @ 5m/s and 2m bin size [4]	±5.0cm/s	±2.6cm/s
Resolution	0.1cm/s	0.1cm/s
Cell Sizes	10 to 800cm	10 to 800cm
Acoustic		
Center Frequency	614.4kHz	614.4kHz
Source Level (re 1µPa)	207dB	204dB
1-Way Beam Width	2.2°	3.8°
Number of Beams	4 (phased array)	4
Beam Angle	30°	30°
Bandwidth (nominal)	6.25% of center frequency	25% of center frequency
Depth Rating		
	300m/1000m (based on configuration)	1000m/4000m based on configuration

[1] @ 5°C and 35 ppt salinity, 24V input.
[2] When mounted with beam 3 at 45°. Also, for platforms with forward velocity higher than reverse (or vice versa) the maximum velocity can be increased 4.75 m/s for bottom track via a firmware command.
[3] Maximum range may be reduced due to flow noise.
[4] Standard deviation refers to single-ping horizontal velocity, specified at half the maximum altitude.
[5] Electronics platform designed to interface with stated 3rd party sensors.
[6] ECCN 6A001 export license required outside US.
[7] ECCN 6A991 export license-free option.

B.4 GPS - Adafruit Ultimate GPS Breakout

2.6 Specification List

	Description
GPS Solution	MTK MT3339
Frequency	L1, 1575.42MHz
Sensitivity[1]	Acquisition: -148dBm, cold start Reacquisition: -163dBm, Hot start Tracking: -165dBm
Channel	66 channels
TTFF	Hot start: 1 second typical Warm start: 33 seconds typical Cold start: 35 seconds typical (No. of SVs>4, C/N>40dB, PDop<1.5)
Position Accuracy	Without aid:3.0m (50% CEP) DGPS(SBAS(WAAS,EGNOS,MSAS)):2.5m (50% CEP)
Velocity Accuracy	Without aid : 0.1m/s DGPS(SBAS(WAAS,EGNOS,MSAS,GAGAN)):0.05m/s
Timing Accuracy (1PPS Output)	10 ns(Typical)
Altitude	Maximum 18,000m (60,000 feet)
Velocity	Maximum 515m/s (1000 knots)
Acceleration	Maximum 4G
Update Rate	1Hz (default), maximum 10Hz
Baud Rate	9600 bps (default)
DGPS	SBAS(defult) [WAAS, EGNOS, MSAS,GAGAN]
QZSS	Support(Ranging)
AGPS	Support
Power Supply	VCC：3.0V to 4.3V；VBACKUP：2.0V to 4.3V
Current Consumption	25mA acquisition, 20mA tracking
Working Temperature	-40 °C to +85 °C
Dimension	16 x 16x 4.7mm, SMD
Weight	**4g**

B.5 IMU+COMPASS - ADIS16488 AMLZ

ADIS16488 Data Sheet

SPECIFICATIONS

T_A = 25°C, VDD = 3.3 V, angular rate = 0°/sec, dynamic range = ±450°/sec ± 1 *g*, 300 mbar to 1100 mbar, unless otherwise noted.

Table 1.

Parameter	Test Conditions/Comments	Min	Typ	Max	Unit
GYROSCOPES					
Dynamic Range		±450		±480	°/sec
Sensitivity	x_GYRO_OUT and x_GYRO_LOW (32-bit)		3.052×10^{-7}		°/sec/LSB
Repeatability[1]	−40°C ≤ T_A ≤ +70°C			±1	%
Sensitivity Temperature Coefficient	−40°C ≤ T_A ≤ +70°C, 1 σ		±35		ppm/°C
Misalignment	Axis-to-axis		±0.05		Degrees
	Axis-to-frame (package)		±1.0		Degrees
Nonlinearity	Best-fit straight line, FS = 450°/sec		0.01		% of FS
Bias Repeatability[1, 2]	−40°C ≤ T_A ≤ +70°C, 1 σ		±0.2		°/sec
In-Run Bias Stability	1 σ		6.25		°/hr
Angular Random Walk	1 σ		0.3		°/√hr
Bias Temperature Coefficient	−40°C ≤ T_A ≤ +70°C, 1 σ		±0.0025		°/sec/°C
Linear Acceleration Effect on Bias	Any axis, 1 σ (CONFIG[7] = 1)		0.009		°/sec/*g*
Output Noise	No filtering		0.16		°/sec rms
Rate Noise Density	f = 25 Hz, no filtering		0.0066		°/sec/√Hz rms
3 dB Bandwidth			330		Hz
Sensor Resonant Frequency			18		kHz
ACCELEROMETERS	Each axis				
Dynamic Range		±18			*g*
Sensitivity	x_ACCL_OUT and x_ACCL_LOW (32-bit)		1.221×10^{-8}		*g*/LSB
Repeatability[1]	−40°C ≤ T_A ≤ +70°C			±0.5	%
Sensitivity Temperature Coefficient	−40°C ≤ T_A ≤ +70°C, 1 σ		±25		ppm/°C
Misalignment	Axis-to-axis		±0.035		Degrees
	Axis-to-frame (package)		±1.0		Degrees
Nonlinearity	Best-fit straight line, ±10 *g*		0.1		% of FS
	Best-fit straight line, ±18 *g*		0.5		% of FS
Bias Repeatability[1, 2]	−40°C ≤ T_A ≤ +70°C, 1 σ		±16		m*g*
In-Run Bias Stability	1 σ		0.1		m*g*
Velocity Random Walk	1 σ		0.029		m/sec/√hr
Bias Temperature Coefficient	−40°C ≤ T_A ≤ +85°C		±0.1		m*g*/°C
Output Noise	No filtering		1.5		m*g* rms
Noise Density	f = 25 Hz, no filtering		0.067		m*g*/√Hz rms
3 dB Bandwidth			330		Hz
Sensor Resonant Frequency			5.5		kHz
MAGNETOMETER					
Dynamic Range		±2.5			gauss
Sensitivity			0.1		mgauss/LSB
Initial Sensitivity Tolerance				±2	%
Sensitivity Temperature Coefficient	1 σ		275		ppm/°C
Misalignment	Axis to axis		0.25		Degrees
	Axis to frame (package)		0.5		Degrees
Nonlinearity	Best fit straight line		0.5		% of FS
Initial Bias Error	0 gauss stimulus		±15		mgauss
Bias Temperature Coefficient	−40°C ≤ T_A ≤ +85°C, 1 σ		0.3		mgauss/°C
Output Noise	No filtering		0.45		mgauss
Noise Density	f = 25 Hz, no filtering		0.054		mgauss/√Hz
3 dB Bandwidth			330		Hz

B.6 Cameras - AVT Manta G-283C

Allied Vision

GigE Vision

Manta

G-283

- Versatile 2.8 Megapixel camera
- 30.4 fps @ full resolution
- PoE option
- Video-iris lens control

Description

GigE camera with Sony ICX674 sensor

Manta G-283B/G-283C includes an 2/3'' Sony ICX674 CCD sensor with EXview HAD II technology. This sensor is distinguished by reduced smear, higher quantum efficiency, and enhanced NIR sensitivity. At full resolution, this camera runs at 30.4 frames per second. This camera with its ICX674 sensor has an excellent image quality even under challenging light conditions.
Options

- Power over Ethernet (PoE)
- Various IR cut/pass filters and lens mounts
- White medical housing

See the#Modular Concept#for lens mount, housing variants, optical filters, case design, and other modular options.

Specifications

Manta	G-283
Interface	IEEE 802.3 1000BASE-T, IEEE 802.3af (PoE) optional
Resolution	1936 (H) × 1458 (V)
Sensor	Sony ICX674
Sensor type	CCD Progressive
Cell size	4.54 µm x 4.54 µm
Lens mount	C-Mount
Max frame rate at full resolution	30.4 fps
ADC	12 bit
Image buffer (RAM)	128 MByte

Manta	G-283
Output	
Bit depth	8/14-8/12 bit
Mono modes	Mono8, Mono12Packed, Mono12
Color modes YUV	YUV411Packed, YUV422Packed, YUV444Packed
Color modes RGB	RGB8Packed, BGR8Packed
Raw modes	BayerRG8, BayerRG12, BayerRG12Packed
General purpose inputs/outputs (GPIOs)	
Opto-isolated I/Os	2 inputs, 2 outputs
RS-232	1
Operating conditions/dimensions	
Operating temperature	+5 °C to +45 °C ambient (without condensation)
Power requirements (DC)	8 to 30 VDC; PoE
Power consumption (@12 V)	3.7 W @ 12 VDC; 4.3 W PoE
Mass	190 g; 200 g (PoE)
Body dimensions (L × W × H in mm)	86.4 × 44 × 29 (including connectors)
Regulations	CE, RoHS, REACH, WEEE, FCC, ICES

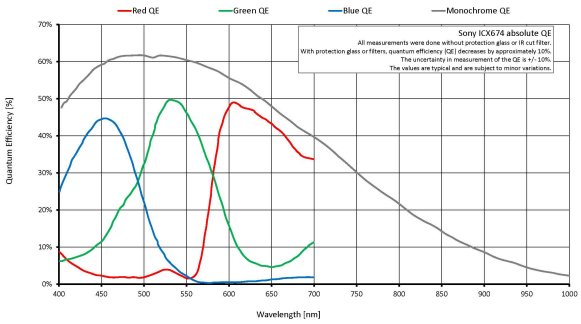

Features

Manta G-283B/G-283C features include:

- Precision Time Protocol (IEEE 1588)
- Camera temperature monitoring

Bibliography

Allotta B.; Caiti, A.; Costanzi R.; Fanelli F.; Fenucci D.; Meli E.; Ridolfi A. (2016). "A new AUV navigation system exploiting unscented Kalman filter". In: *IEEE Journal of Oceanic Engineering*.

Allotta B.; Bartolini, F.; Caiti A.; Costanzi R.; Di Corato F.; Fenucci D.; Gelli J.; Guerrini P.; Monni N.; Munafò A.; Natalini M.; Pugi L.; Ridolfi A.; Potter J. R. (2015). "Typhoon at CommsNet13: Experimental experience on AUV navigation and localization". In: *Annual Reviews in Control*.

Beiter S.; Guidance, K.; Corp N.; Poquette R. (1998). "Precision Hybrid Navigation System for Varied Marine Applications". In: *Position Location and Navigation Symposium, IEEE*, pp. 316 –323. DOI: 10.1109/PLANS.1998.670106.

Bit, Fundació (2014). *Estrategia de Innovación para la Especialización Inteligente RIS3. Diagnóstico de Especialización Económica, Tecnológica y Científica de las Islas Baleares*.

Bonin-Font Francisco; Cosic, Aleksandar; Negre Pep Lluis; Solbach Markus; Oliver Gabriel (2015). "Stereo SLAM for robust dense 3D reconstruction of underwater environments". In: *MTS/IEEE OCEANS 2015 - Genova: Discovering Sustainable Ocean Energy for a New World*.

Bonin-Font F.; Massot, M.; Oliver G. (2016). "Towards Visual Detection , Mapping and Quantification of Posidonia Oceanica using a Lightweight AUV". In: *10th IFAC Conference on Control Applications in Marine Systems*.

Burguera A.; Bonin-Font, F.; Oliver G. (2016a). *ARSEA Project*. URL: http://srv.uib.es/arsea/.

Burguera Antoni; Bonin-font, Francisco; Lisani Jose Luis; Petro Ana Belen; Oliver Gabriel (2016b). "Towards Automatic Visual Sea Grass Detection in Underwater Areas of Ecological Interest". In: *IEEE International Conference on Emerging Technologies and Factory Automation, Berlin*.

Caiti, Andrea et al. (2014). "Experimental results with a mixed USBL / LBL system for AUV navigation". In: *Underwater Communications and Networking (UComms)*, pp. 1 –4.

Caiti A.; Calabro, V.; Di Corato F.; Fabbri T.; Fenucci D.; Munafo A.; Allotta B.; Bartolini F.; Costanzi R.; Gelli J.; Monni N.; Natalini M.; Pugi L.; Ridolfi A. (2014). "Thesaurus: AUV teams for archaeological search. Field results on acoustic communication and localization with the Typhoon". In: *2014 22nd Mediterranean Conference on Control and Automation, MED* 22, pp. 857–863.

Carreras M.; Candela, C.; Ribas D.; Mallios A.; Magí L.; Vidal E.; Palomeras N.; Ridao P. (2013). "SPARUS II, Design of a Lightweight Hovering AUV". In: *Fifth International Workshop in Marine Technology (MARTECH)*.

Chao Liu; Wang, Meng (2010). "Removal of water scattering". In: *ICCET - International Conference on Computer Engineering and Technology, Proceedings*.

Chen Ling; Wang, Sen; Hu Huosheng; Gu Dongbing; Liao Liqing (2015). "Improving Localization Accuracy for an Underwater Robot with a Slow-Sampling Sonar Through Graph Optimization". In: *IEEE Sensors Journal* 15 (9), pp. 5024–5035.

Chiang John Y.; Chen, Ying Ching (2012). "Underwater image enhancement by wavelength compensation and dehazing". In: *IEEE Transactions on Image Processing*.

Di Corato F.; Fenucci, D.; Caiti A.; Costanzi R.; Monni N.; Pugi L.; Ridolfi A.; Allotta B. (2014). "Toward underwater acoustic-based simultaneous localization and mapping. Experimental results with the Typhoon AUV at CommsNet13 sea trial". In: *2014 Oceans - St. John's, OCEANS 2014*.

Dormer, Murray (2014). *Global Market Prospects. Presented at UUV Oceanology International London. Extracted from the Douglas Westwood World AUV Market Report*.

Díaz-Almela Elena; Duarte, Carlos M. (2008). "MANAGEMENT of Natura 2000 habitats : Posidonia beds (Posidonion oceanicae) 1120". In: *Technical Report*.

Eustice R.M.; Pizarro, O.; Hanumant S. (2008). "Visually Augmented Navigation for Autonomous Underwater Vehicles". In: *IEEE Journal of Oceanic Engineering* 33, pp. 103–122.

Felemban Emad; Shaikh, Faisal Karim; Qureshi Umair Mujtaba; Sheikh Adil A.; Qaisar Saad Bin (2015). "Underwater Sensor Network Applications: A Comprehensive Survey". In: *International Journal of Distributed Sensor Networks*.

Fengzhong Q U; Shiyuan, Wang; Zhihui W U; Zubin L I U (2016). "A survey of ranging algorithms and localization schemes in underwater acoustic sensor network". In: *China Communications* 13 (3), pp. 66 –81.

Fidalgo E.; Ortiz, A.;Bonnin-Pascual F.; Company J.P. (2016). "Fast Image Mosaicing using Incremental Bags of Binary Words". In: *IEEE International Conference on Robotics and Automation (ICRA)*.

Galdran Adrian; Pardo, David; Picón Artzai; Alvarez-Gila Aitor (2015). "Automatic Red-Channel underwater image restoration". In: *Journal of Visual Communication and Image Representation*.

Gordon N.J.; Salmond, D.J.; Smith A.F.M. (1993). "Novel approach to nonlinear/non-Gaussian Bayesian state estimation". In: *IEEE Proceedings F Radar and Signal Processing*.

Illes Balears, Govern de les (2012). *Pla de Ciència, Tecnologia,Innovació i Emprenedoria deles Illes Balears 2013-2017*.

Jordà Gabriel; Marbà, Núria; Duarte Carlos M. (2012). "Mediterranean seagrass vulnerable to regional climate warming". In: *Nature Climate Change*.

Jourdan D. ; Brown, B. (1997). "Improved navigation system for USBL users". In: *Oceans '97. MTS/IEEE Conference Proceedings* 1, pp. 727–735.

Julier Simon J.; Uhlmann, Jeffrey K (1997). "A new extension of the Kalman filter to nonlinear systems". In: *Int Symp AerospaceDefense Sensing Simul and Controls*, pp. 182–193.

Kalman, R.E. (1960). "A new approach to linear filtering and prediction problems". In: *Journal of basic Engineering* 82.1, pp. 35–45.

Kaushal Hemani; Georges, Kaddoum (2016). "Underwater Optical Wireless Communication". In: *IEEE Access* 4, pp. 1518 –1547.

Kebkal Konstantin G.; Kebkal, Oleksiy G.; Bannasch-Rudolf; Yakovlev Sergey G. (2012). "Performance of a combined USBL positioning and communication system using S2C technology". In: *Program Book - OCEANS 2012 MTS/IEEE Yeosu: The Living Ocean and Coast - Diversity of Resources and Sustainable Activities*.

Kebkal Konstantin G.; Bannasch, Rudolf (2002). "Sweep-spread carrier for underwater communication over acoustic channels with strong multipath propagation". In: *The Journal of the Acoustical Society of America*, pp. 2043–2052.

Lysanov, L.M. Brekhovskikh; Yu.P. (2001). *Fundamentals of Ocean Acoustics*. Springer. ISBN: 0387954678.

Massot M.; Bonin-Font, F.; Negre P.Ll.; Guerrero E.; Martorell A.; Oliver G. (2016). "A 3D Mapping, Obstacle Avoidance and Acoustic Communication Payload for the AUV SPARUS II". In: *Seventh International Workshop in Marine Technology (MARTECH)*.

Moore T. ; Stouch, D. (2014). "A Generalized Extended Kalman Filter Implementation for the Robot Operating System". In: *Proceedings of the 13th International Conference on Intelligent Autonomous Systems (IAS-13)*. Springer.

— (2016). "A Generalized Extended Kalman Filter Implementation for the Robot Operating System". In: *Advances in Intelligent Systems and Computing* 302, pp. 335–348.

Mur-Artal R.; Montiel, J.M.; Tardós J.D. (2015). "ORB-SLAM: a Versatile and Accurate Monocular SLAM System". In: *IEEE Transactions on Robotics* 31.5, pp. 1147–1163.

Negre P.L.; Bonin-font, F.; Oliver G. (2016). "Cluster-based loop closing detection for underwater slam in feature-poor regions". In: *IEEE International Conference on Robotics and Automation (ICRA)*.

Palomeras N.; El-Fakdi, A.; Carreras M.; Ridao P. (2012). "COLA2: A Control Architecture for AUVs". In: *IEEE Journal of Oceanic Engineering* 37.4, pp. 695–716. ISSN: 03649059. DOI: 10.1109/JOE.2012.2205638.

Philip, D R C (2003a). "An evaluation of USBL and SBL acoustic systems and the optimisation of methods of calibration - Part 1". In: *The Hydrographic Journal* 108, pp. 18–25.

— (2003b). "An evaluation of USBL and SBL acoustic systems and the optimisation of methods of calibration - Part 2". In: *The Hydrographic Journal* 109, pp. 10–20.
— (2003c). "An evaluation of USBL and SBL acoustic systems and the optimisation of methods of calibration - Part 3". In: *The Hydrographic Journal* 110, pp. 11–19.
Prats M.; Perez, J.; Fernandez J.J.; Sanz P.J. (2012). "An Open Source Tool for Simulation and Supervision of Underwater Intervention Missions". In: *Proceedings of the IEEE/RSJ International Conference on Intelligent Robots and Systems (IROS)*, pp. 2577–2582. URL: http://www.irs.uji.es/uwsim/.
Quigley M.; Conley, K.; Gerkey B.P.; Faust J.; Foote T.; Leibs J.; Wheeler R.; Ng A. Y. (2009). "ROS: an Open Source Robot Operating System". In: *ICRA Workshop on Open Source Software*.
Reuters (2014). *Research and Markets: Global Unmanned Underwater Vehicles Market 2014-2019: ROV and AUV Vehicles for Defense, Oil and Gas & Scientific Research*.
Ribas David; Palomeras, Narcis; Ridao Pere; Carreras Marc; Mallios Angelos (2012a). "Girona 500 AUV: From Survey to Intervention". In: *IEEE/ASME Transactions on Mechatronics*.
Ribas D.; Ridao, P.; Mallios A.; Palomeras N. (2012b). "Delayed State Information Filter for USBL-Aided AUV Navigation". In: *Proceedings of IEEE International Conference on Robotics and Automation (ICRA)*. Minnesota (USA).
Ridao Pere; Ribas, David; Hernàndez Emili; Rusu Alex (2011). "USBL/DVL navigation through delayed position fixes". In: *Proceedings - IEEE International Conference on Robotics and Automation*.
Ridao P.; Sanz, P.J.; Oliver G. (2016). *MERBOTS Project*. URL: http://www.irs.uji.es/merbots/consortium.
Rigby Paul; Pizarro, Oscar; Williams Stefan B. (2006). "Towards Geo-Referenced AUV Navigation Through Fusion of USBL and DVL Measurements". In: *IEEE Journal of Oceanic Engineering*.
Sun Dajun; Zheng, Cuie; Yeng Jun; Wu Yongting (2014). "Initial study on the precision evaluation for ultra short baseline positioning system". In: *2014 Oceans - St. John's*, pp. 1 –7.
Thrun S.; Burgard, W.; Fox D. (2005). *Probabilistic Robotics (Intelligent Robotics and Autonomous Agents)*. The MIT Press. ISBN: 0262201623.
Wan E.A.; Van Der Merwe, R. (2000). "The unscented Kalman filter for nonlinear estimation". In: *IEEE Adaptive Systems for Signal Processing, Communications, and Control Symposium 2000. AS-SPCC*. Pp. 153–158.
Whitcomb L.; Yoerger, D.; Singh H. (1999). "Advances in Doppler-Based Navigation of Underwater Robotic Vehicles". In: *Proceedings 1999 IEEE International Conference on Robotics and Automation*, pp. 399 –406.
Wiener, N. (1949). *Extrapolation, Interpolation and Smoothing of Stationary Time Series with Engineering Applications*. New York: Technology Press and John Wiley & Sons, Inc.
Willemenot E.; Morvan, P.Y.; Pelletier H.; Hoof A.; (2009). "Subsea Positioning by Merging Inertial and Acoustic Technologies". In: *OCEANS '09 IEEE Bremen: Balancing Technology with Future Needs* 1. DOI: 10.1109/OCEANSE.2009.5278162.
Zhang Fumin; Marani, Giacomo; Smith Ryan N.; Choi Hyun Taek (2015). "Future trends in marine robotics". In: *IEEE Robotics and Automation Magazine*.